Anaerobic biodegradation of Miocene lignites from an opencast mine by autochthonous microorganisms stimulated under laboratory conditions

Michał Bucha[1], Piotr Siupka[2], Anna Detman-Ignatowska[3], Sushmita Deb[1], Agnieszka Bylina[6], Daria Kaim[2], Aleksandra Chojnacka[4], Dominika Kufka[5], Dominika Lewicka-Szczebak[1], Anna Sikora[3], Leszek Marynowski[6]

[1]Institute of Geological Sciences, University of Wrocław, Wrocław, 50-205, Poland
[2]Institute of Biology, Biotechnology and Environmental Protection, University of Silesia in Katowice, Katowice, 40-031, Poland
[3]Institute of Biochemistry and Biophysics, Polish Academy of Sciences, Warszawa, 02-106, Poland
[4]Institute of Biology, Warsaw University of Life Sciences, Warszawa, 02-776, Poland
[5]„Poltegor – Instytut" Opencast Mining Institute, Wrocław, 51-616, Poland
[6]Institute of Earth Sciences, University of Silesia in Katowice, Sosnowiec, 41-200, Poland

Correspondence to: Michał Bucha (michal.bucha@uwr.edu.plm)

Abstract. The supplementation and provision of appropriate nutrients to microorganisms, which are often lacking in the natural environment are essential and critical for microbial growth. One such element is nitrogen, most of which is found in the Earth's atmosphere. In this study, we present evidence of nitrogen processing and anaerobic N_2-fixation by microorganisms naturally present in sedimentary organic matter. Miocene detritic lignite from the opencast mine was incubated under anaerobic conditions in the dark (headspace atmosphere 85% N_2, 10% CO_2, 5% H_2) for three years. The natural microbial community of these coal materials was stimulated for growth through the addition of trace elements, vitamins, and carbon-bearing compounds such as yeast extract, nutrient broth, methanol, and sodium acetate. A visual indicator of microbial activity was observed as the color of the fermentation solutions changed over time: from colorless to light yellow (after 3 months), dark brown (after 6 months), and finally black (after more than 1 year). This progression suggests the dissolution of fulvic and humic acids. At the end of the cultivation period, the total nitrogen (TN) and total inorganic nitrogen (TIN) contents in the solutions were significantly reduced whereas in incubations with sodium acetate, total organic nitrogen (TON) content significantly increased compared to the initial levels. In most cases, total carbon (TC) content significantly increased due to biodegradation, except for the incubations where methanol was added. A GC-MS analysis of the total extracts from lignite revealed that the main macromolecule decomposed by microorganisms was lignin, along with its diagenetic derivatives. The biogas released during the process contained CO_2 and trace amounts of CH_4 (up to 50 ppm). Isotopic data indicated the occurrence of anaerobic CH_4 oxidation. Notably, 16S rRNA gene sequencing identified the presence of N_2-fixing microorganisms in all investigated samples, members of the order *Rhizobiales* (families *Beijerinckiaceae*, *Rhizobiaceae*). Our findings demonstrate that N_2-fixation may play a pivotal role in coal decomposition under anaerobic conditions.

1 Introduction

35 Organic-rich sediments, including coals, are habitats for microorganisms such as Bacteria, Archaea, and Fungi. Coal decomposition processes under aerobic and anaerobic conditions are widely studied to better understand the formation of microbial gases rich in CH_4 and H_2 (Vinson et al., 2017). Stimulation of natural microbial communities from organic-rich habitats can result in the formation of coal bed methane (CBM), which is a biotechnological method alternative to traditional industrial processes of methane production (Fallgren et al., 2013; Pytlak et al., 2021; Ritter et al., 2015; Singh et al. 2012;

40 Strąpoć et al., 2011). For these reasons, carbon cycling in organic-rich environments is studied in detail, while nitrogen cycling in coal-bearing strata is a relatively rarely undertaken research topic (Flores and Moore, 2024). The positive exception is the monitoring of NOx emissions from the combustion of lignite or hard coal (Scheffknecht et al., 2011). The lack of proper studies of nitrogen cycling in coal environments is mainly caused by very low nitrogen content in the coal matrix (which is usually lower than 2%) (Nelson et al., 1992). However, nitrogen cycling is the second most important element after carbon in

45 controlling the natural diversity, dynamics, and functioning of marine, freshwater, and terrestrial ecosystems (Stankiewicz and Van Bergen, 1998).

The main pool of nitrogen on Earth is the atmosphere, which contains 99.96% of total nitrogen as gaseous N_2. The remaining 0.04% is the nitrogen bound in organic (57%) and inorganic form (43%) (Stankiewicz and Van Bergen, 1998). Organic nitrogen occurs in living biomass of terrestrial and aquatic origin and products of its decomposition as sedimentary organic

50 matter (OM). The nitrogen cycle is complex, and identification of transformations of nitrogen compounds in OM is very difficult and requires sophisticated analytical methods, e.g. stable isotope studies (Deb et al., 2024; Müller et al., 2014). However, many questions remain to be answered, especially when considering N_2O and N_2 fluxes from anthropogenic sources or natural habitats (e.g., peatlands, wetlands) (Yu et al., 2020). Recently, it was found that heterotrophic nitrification, a process where nitrites and N_2O are produced during the decomposition of soil OM, may play an important or even a dominant role in

55 N_2O emissions (Lewicka-Szczebak et al., 2021; Zhang et al., 2015), however this process has been often ignored in nitrogen balance. Hence, the combined studies of OM decomposition and nitrogen transformations may open new insights into soil N cycling. Processes such as N_2-fixiation, denitrification, nitrification, dissimilatory nitrate reduction to ammonium (DNRA), and anaerobic ammonium oxidation (ANNAMOX) occur commonly in many environments (Müller and Clough, 2014).

The main forms of nitrogen in sedimentary OM are biomolecular structures proteins (e.g., collagen, keratins, myosin), amino acids (as DNA, RNA), amino sugar polymers (e.g., chitin – N-containing polysaccharide) or other N-containing macromolecules (e.g., porphyrins). Proteins and amino acids are easily degraded by microorganisms and they are relatively unstable during deposition and later after diagenesis. Moreover, chitin and porphyrins, much more resistant N-containing materials, are minor contributors to the nitrogen in the bio- and geosphere. Nitrogen is often linked with aromatic structures of non-labile fractions of OM (Haynes, 2000). Lignin may contain nitrogen in its structure, e.g. as –NCH_3 groups (Whitehead and Quicke, 1960). In summary, in many organic-rich sediments, the total amount of nitrogen is very low. For example, Miocene lignites from Konin and Bełchatów (Poland) contain 0.2 to 0.6% nitrogen (Bucha et al., 2020; Kwiatos et al., 2018). Moreover, N content is up to two or three times higher in detritic lignites than in xylites, due to a higher proportion of lignin to cellulose.

The decomposition of any OM is slowed if the C:N ratio is >30 (Mortier et al., 2016). Thus, the bioavailability of nitrogen in coal habitats is a limiting factor for the growth of microorganisms like in many oligotrophic environments (Strąpoć et al., 2011). Leschine et al. (1989) discovered the bacteria able for lignocellulose degradation and anaerobic N_2-fixation. Dey et al. (2021) showed that N_2-fixing bacteria are active under anaerobic conditions and use humic substances as extracellular electron mediators. This discovery indicates that bacteria can fix nitrogen not only in an oxygen-rich atmosphere. It seems that microorganisms adapt to conditions and sources of biophilic elements. In soils N_2-fixing bacteria called rhizobia can form a symbiotic relationship with legumes. The result of this symbiosis is forming the nodules on the plant root, within which the bacteria can convert atmospheric nitrogen into ammonia that can be used by the plant. Recent studies revealed microorganisms able for nitrogen processing in coal-rich sediments. Guo et al. (2015) detected the microbial taxa related to N metabolism in Chinese coals, including N_2-fixing taxa and denitrifying taxa. Shi et al. (2021) found that microbial N metabolism affected OM decomposition in coals such as the decomposition of cellulose and carbohydrate. Therefore, it is very important to better understand the role of nitrogen cycling (especially N_2-fixing), and lignocellulose degradation under anaerobic conditions.

In this work, we show the evidence of anaerobic activity of N_2-fixing microorganisms that naturally occurred in Miocene detritic coals from Poland. The basic microbiological studies are supplemented with geochemical data, including biogas composition, elemental content of fermentation liquids as well as GC-MS studies of degraded coals. The results of 16S rRNA

amplicon sequencing of microbiological samples from the experimental coals and coals without any cultivation were compared

85   to prove N_2-fixing bacteria activity under anaerobic conditions during coal degradation. The novelty of this work is the

simulation of natural OM decomposition by maintaining anaerobic conditions of lignite cultivation for a few years and the

stimulation of microorganisms naturally occurring in raw lignite samples. Geochemical and microbiological methods were

used to prove anaerobic N_2-fixation in lignite deposits for the first time.

2 Materials and methods

90   ### 2.1 Sample collection and separation

The Miocene detritic lignite used for this study was collected in 2019 from the mine "PAK Kopalnia Węgla Brunatnego Konin"

located in central Poland. The name of the open pit was "Jóźwin IIB" (location coordinates: 52° 24.781′N, 18° 10.150′E). The

lignite deposits in this basin are characterised as immature and at the stage of microbial conversion and early diagenesis. The

huminite reflectance in these lignites ranges from 0.16 to 0.20% (average 0.19%) (Fabiańska, 2007; Fabiańska and Kurkiewicz,

95   2013). The deposits consist mainly of the detritic lithotype with xylite fragments. The geology, geochemistry, and

sedimentology of this deposit were described elsewhere (Bechtel et al., 2020, 2019; Fabiańska and Kurkiewicz, 2013;

Marynowski et al., 2021; Widera, 2016; Widera et al., 2017, 2021; Zieliński and Widera, 2020).

Large chunks of coal were gently collected from the freshly exploited wall of the outcrop and stored during transportation in

the glass jars flushed with nitrogen. On the same day coal samples were placed in the Vinyl Anaerobic Chamber (Coy

100   Laboratory Products, Inc, and the next steps were performed at the anaerobic atmosphere (N_2 85%, CO_2 10%, H_2 5%). The

next day the coal was crushed into small particles (c.a. 1x1 cm), using metal, sterile tools under the glove box, and only the

middle part of the coal was used as a material for cultivation.

2.2 Experimental setup

In each serum bottle (250 mL) around 10 g of coal material was placed. A modified, sterilised M9 minimal mineral medium

105   (Miller, 1972), where $MgSO_4$ was replaced by $MgCl_2$ (190 mg/L), was added in a volume of 150 mL.. No glucose was added.

The pH was 7. Yeast extract and nutrient broth (BTL Sp. z o.o., Department of Enzymes and Peptydes, Łodź, Poland) were

later added to some of the cultivations as sources of vitamins, peptones, and enzymes (Zinder, n.d.1993); the concentrations of both equaled 100 mg/L The M9 minimal medium was supplemented with trace mineral solution (modified Wolin's mineral solution; DSMZ Germany, Media No. 826) for half of the cultivations (MG, MGA, MGB, MGC, MGD, MGE). Carbon-

110 bearing compounds (methanol, sodium acetate, or their mixtures) were used as microbial stimulants for enrichment of native microorganisms. No additional inoculum was added to the bottles. Therefore, we expected stimulation of native microorganisms present on and inside coal particles. The scheme of the repetitions and carbon-bearing additives used for cultivation (stimulation of autochthonous microflora) are presented in Table 1.

Table 1: Experimental setup of the lignite cultivation (bold font – variants selected for microbiome structure profiling).

Name	Lignite [g]	M9 minimal media [mL]	Trace solution [mL]	Yeast extract [mg/L]	Nutrient broth [mg/L]	Sodium acetate [mg/L]	Methanol [mg/L]	Repetitions
M9	10	150						2
M9A	10	150		100				2
M9B	10	150			100			2
M9C	10	150		100	100			2
M9D	10	150		100	100	2500		2
M9E	10	150		100	100		2100	2
MG	10	150	1					2
MGA	10	150	1	100				2
MGB	10	150	1		100			2
MGC	10	150	1	100	100			2
MGD	10	150	1	100	100	2500		2
MGE	10	150	1	100	100		2100	2

115

After preparation, the batch cultivation bottles were stored at 20°C in the dark for 3 years. To avoid potential leakage of the headspace gas through the septa and caps, the bottles were placed upside down, with the caps at the bottom. They were never opened, and only biogas was collected from four bottles after 1st year and from each of the bottles after 3rd year of cultivation. That strategy allowing the microorganisms to remain in stable, undisturbed conditions without any additional interventions.

120 The main aim of this task was to simulate conditions of stable anoxic environments, where the possible sources of OM are limited or limited to the minimum without any interference in the cultivation of the lignite samples.

2.3 Analyses of biogas

The chromatographic system described in this paper was built based on Shimadzu Gas Chromatograph Nexis 2030. The used model was equipped with two parallel detectors – a barrier ion discharge detector (BID) and a thermal conductivity detector (TCD). Each sample in the volume of 1 mL was manually injected into the split/splitless injector using an SGE chromatographic syringe with a gas valve. The injected sample was then divided between two porous layers open tubular capillary columns filled molecular sieve 5A (RT-MSieve 5A 30 m x 0.32 mm x 30 μm, Restek, USA, #19722) and fused silica (Carboxen 1010 PLOT 30 m x 0.53 mm x 0.30 μm, Supelco, USA, #25467).

The dimensions of the columns were selected to achieve a splitting ratio of 1:5, directing most of the sample to the column Carboxen 1010 PLOT and BID detector. Corresponding calculations were made in Shimadzu AFT (Advanced Flow Technology) software. The concentration of O_2 and N_2 was measured using a TCD with RT-Msieve 5A column, where a trace concentration of CH_4 was detected using a BID detector equipped with Carboxen 1010 PLOT column. The details regarding the chromatographic system used for this study are presented elsewhere (Bucha et al., 2025).

The isotopic composition of carbon from CH_4 and CO_2 was analyzed using the Picarro G2201-i Isotopic Analyzer. The precision error for $\delta^{13}C(CH_4)$ was less than 0.55‰ and in the case of $\delta^{13}C(CO_2)$, less than 0.16‰.

2.4 Analyses of fermentation liquids

Fermentation liquids were analysed using Multi NC Analyzer 2100. For each sample, 8 mL were placed in the glass vials and 500 microliters of them were transferred by the autosampler to the analyser. The sample was firstly transferred to a catalytic reactor and later combusted in the presence of O_2 at 800°C. The carbon concentration was measured using a nondispersive infrared sensor (NDIR), whereas nitrogen concentration using electrochemical detector (CHD). Total carbon (TC) and total nitrogen content (TN) were calculated according to calibration curves using saccharose and potassium nitrate (TN). The mean standard deviation for the TC and TN was 1.66 mg/L and 0.11 mg/L, respectively.

Further, for analysis of nitrate (NO_3^-) and ammonium (NH_4^+) concentrations in the cultured samples, the media from the crimped bottles was drawn out using a syringe and measured using the SLANDI Photometer LF300. It is a versatile instrument designed for water and wastewater analysis at various wavelengths (ranging from 380 nm to 810 nm). Since the media was

very dark in colour, the samples were diluted to ensure accurate photometric measurements. Special kits dedicated for measurements of NO_3^- (Slandi, cat. no. ZW 20342) and NH_4^+ (Slandi, cat. no. ZW 20212) were used for sample preparation. Following a standardized protocol, we added specific reagents (Reagent A and Reagent B, not specified by the manufacturer) to the diluted media, waited for the reactions to develop colour, and measured the concentrations photometrically. For our

150   analysis, the photometer automatically selected 610 nm for NH_4^+ and 520 nm for NO_3^- concentrations.

The total inorganic nitrogen (TIN) was calculated as the sum of nitrogen from nitrates and ammonia in the solution. Moreover, for the solution samples at the end of cultivation gaseous N_2 in a maximal concentration of 20 mg/L was included for the calculations. The total organic nitrogen (TON) was calculated from the difference between TN and TIN.

The pH was measured using a WTW electrode. Electrical conductivity (EC) was measured using the stationary Mettler Toledo

155   S230 Seven Compact conductivity meter. Both parameters were measured at the beginning and end of incubation. Measurements in the intermediate period were not performed in order not to excessively interfere with the stability of incubation in the dark.

2.5 GC-MS analyses of the lignite extracts

Samples of the decomposed lignite OM were separated from the solution and frozen at -20°C, then lyophilized, where raw

160   samples from the mine were dried at room temperature before further processing. After crushing around 1 g of the sample was extracted using a dichloromethane (DCM)/methanol mixture (1:1 v:v) with an accelerated Dionex ASE 350 solvent extractor. All solvents were of spectroscopic grade. Aliquots of total extract (analysis was performed for all samples) were converted to trimethylsilyl (TMS) derivatives by reaction with BSTFA, 1% trimethylchlorosilane, and pyridine for 3 hours at 70 °C. An internal standard (ethyl vanillin, ribonnic acid or trans-cinnamic acid) was added to the total extracts before derivatization. The

165   excess reagent was evaporated under a stream of dry nitrogen gas and the mixture dissolved in an equivalent volume of *n*-hexane. A blank sample (baked silica gel) was analyzed using the same procedure (including extraction and separation on columns).

Gas chromatography-mass spectrometry (GC-MS) analyses were carried out with an Agilent Technologies 7890A gas chromatograph and Agilent 5975C Network mass spectrometer with Triple-Axis Detector (MSD). Helium (6.0 Grade) was

170 used as a carrier gas at a constant flow of 2.6 mL/min. Separation was obtained on a fused silica capillary column (J&W HP5-MS, 60 m x 0.25 mm i.d., 0.25 µm film thickness) coated with a chemically bonded phase (5% phenyl, 95% methylsiloxane), for which the GC oven temperature was programmed from 45 ºC (1 min) to 100 ºC at 20 ºC/min, then to 300 ºC at 3 ºC/min (hold 40 min), with a solvent delay of 10 min.

The GC column outlet was connected directly to the ion source of the MSD. The GC-MS interface was set at 280 ºC, while

175 the ion source and the quadrupole analyzer were set at 230 and 150 ºC, respectively. Mass spectra were recorded from m/z 45–550 (0–40 min) and m/z 50–700 (> 40 min). The MS was operated in the electron impact mode, with an ionization energy of 70 eV. Analysis was performed in the Institute of Earth Sciences, Faculty of Natural Sciences, University of Silesia in Katowice.

Quantification of organic compounds was performed using Openchrome Lablicate version 1.5.0 software and according to the

180 NIST Database.

2.6 Total DNA isolation, 16S rRNA profiling, and functional predictions

The total DNA from raw lignite samples were purified using a house protocol based on several other methods (Alawi et al., 2014; Bag et al., 2016; Narayan et al., 2016; Schulze-Makuch et al., 2018; Töwe et al., 2011). After collection lignites were stored at -80 °C, approx. 5 g of each sample was transferred to beakers under sterile conditions and used for microbial cell

185 extraction. The microbial cell extraction was performed by two washes with Ringer's solution supplemented with 0.5 % Tween (v/v) followed by two washes with cell extraction buffer (1 M NaCl, 1% PEG8000 (w/v), pH 9.2). For each wash samples were mixed with buffer in a 1:10 (w/v) ratio, incubated with shaking at 24 °C, 120 rpm for 25 min followed by centrifugation at 250 x g, 4 °C for 10 min. After each centrifugation supernatants were collected into the sterile beaker and stored on ice until further processing. Next, samples were vacuum filtrated through a sterile 0.22 µm cellulose filter. Filters with gathered material

190 were placed in 15 mL tubes and stored at -80 °C overnight. For cell lysis, sterile glass beads, acid-washed PVPP (Merck), and 6 mL of cell lysis buffer (100 mM Tris-HCl, 20 mM EDTA, 1% SDS (w/v), 0.5 M NaCl, pH 8.0) supplemented with 60 µL of β-mercaptoethanol (Merck) were added to each tube with a filter. Samples were shaken for 15 min at 3000 rpm at room temperature (RT) after which they were cool down on ice for 5 min. 1 mL aliquots of samples were transferred to 2 mL

microcentrifuge tubes and 0.9 mL of buffered phenol:chloroform:isoamyl alcohol (PCI, pH 8.5; Thermo-Fisher Scientific) was

195 added to each aliquot. Samples were mixed on a rotatory mixer for 10 min, 30 rpm at RT followed by centrifugation at 14 000

x g, 4 °C for 10 min. Aqueous fractions were transferred to new 2 mL microcentrifuge tubes and an equal amount of HPLC

grade chloroform (Chem-Lab, Belgium) was added followed by mixing, centrifugation, and aqueous fraction transfer as above.

An equal volume of PEG precipitation solution (1.2 M NaCl, 10% PEG8000 (w/v)) was added to each aliquot followed by a

gentle mix by rotating the tubes and overnight precipitation at 4 °C. Next, samples were centrifugated at 14 000 x g, 4 °C for

200 30 min, supernatant was removed, and pellets were washed twice with 1 mL ice-cold 80% EtOH solution (Merck) followed

by centrifugation at 14 000 x g, 4 °C, 10 min. After the removal of EtOH solution, the pellets were air dried for a few minutes

and 60 μL of Tris buffer (10 mM Tris-HCl, pH 8.5) was added to each sample, followed by re-hydration by incubation on a

rotatory mixer at 30 rpm, RT for overnight. After re-hydration aliquots were merged and 1 μL of glycogen (Thermo-Fisher

Scientific), 0.5 vol. of 7.5 M ammonium acetate (Merck) and 2.5 vol. (sample + ammonium acetate) of absolute EtOH were

205 mixed with each sample followed by overnight incubation at -20 °C for another precipitation and concentration of DNA. After

incubation samples were subjected to EtOH wash and re-hydration as above.

As DNA yield from the samples was expected to be low, the concentration and ability to amplify sequences from the isolated

material was verified by quantitative polymerase chain reaction (qPCR). For this amplification of the 16S rRNA gene fragment

was performed using MF341 (5' CCTACG GGA GGC AGC AG 3') and MR907 (5' CCG TCA ATT CMT TTG AGT TT 3')

210 primers (Markowicz et al., 2021). Reaction was performed using FastStart Essential DNA Green Master Kit (Roche,

Switzerland), each reaction included: 5 μL of SYBR Green Master Mix, 0.5 μL of each primer (10 μM each), 1 μL of a

template, and 3 μL of water. pTZ57R/T vector with target 16S rRNA gene sequence amplified from *Pseudomonas* sp. F8C

was used to prepare a standard curve by making a dilution series (10^{-2} -10^{-10}). As a positive control, *E. coli* genomic DNA was

used as a template, as the negative control the same reaction was prepared but with water instead of the template. Each reaction,

215 standard and control has been made in two technical repeats. The reaction was conducted on LightCycler 96 device (Roche,

Switzerland) with a program: preincubation at 95 °C for 600 s followed by 40 cycles of 95 °C for 10 s, 57 °C for 20 s, 72 °C

for 20 s with single signal reading at the end of each cycle at 81 °C. Cycles were followed by melting curve determination: 95

°C for 10 s, 65 °C for 60 s, followed by continuous signal reading until reaching 95 °C with a 0.5 °C/s temperature ramp.

Results were analysed using LightCycler®96 SW software (version 1.1, Roche, Switzerland). The samples' DNA

220   concentration was based on the standard curve obtained from the dilution series of the qPCR standard.

Total DNAs from the microbial communities grown in serum bottles were extracted and purified using a PowerSoil PRO DNA isolation kit (Qiagen), according to the manufacturer's protocol with some modifications (Detman et al., 2018a). DNA was extracted from 4 mL samples containing a mixture of lignite and fermentation liquid. Samples were centrifuged and pellets were used for DNA extraction. The concentration of purified DNA was [ng/µL] 44,5; 93,3; 265,3; 319,6 for MG, MGC, MGD,

225   and MGE, respectively.

DNA samples from both coal and microbial communities have been sent for amplification, library preparation and sequencing to Genomed S.A. (Warsaw, Poland). The amplification of V3-V4 hypervariable region of 16S rDNA was performer using primers 341F (5' CCTACGGGNGGCWGCAG 3') and 785R (5' GACTACHVGGGTATCTAATCC 3') with Q5 Hot Start High Fidelity 2x Master Mix according to the manufacturer protocol. Paired-end 2x300 bp sequencing was performer on

230   MiSeq platform (Illumina, USA). Resulting sequences were quality controlled using FIGARO (Weinstein et al., 2019) and adaptor sequences as well as short reads filtering (<30 bp) was done with Cutadapt (Martin, 2011).

Sequencing results were analysed using Qiime2 package (version: amplicon2023.9; Bolyen et al., 2019). Reads denoising, merging, dereplication, filtration of chimeras and sequence occurrence frequency were performed with DADA2 package (Callahan et al., 2016). Taxonomy classification of results was done using Qiime2 feature classifier (Bokulich et al., 2018)

235   trained on Greengenes2 (McDonald et al., 2024) database.

All raw sequences generated in this study have been deposited in NCBI's Sequencing Reads Archive (SRA) database with the following accession numbers: BioProject – PRJNA1190450; BioSample – SAMN45045376, SAMN45045377, SAMN45045378, SAMN45045379, SAMN45045380, SAMN45045381, SAMN45045382.

The functional prediction of microbial communities was done using PiCrust2 package (Douglas et al., 2020) with

240   phylogenetical placement done using EPA-NG (Barbera et al., 2019) and gappa (Czech et al., 2020) packages, hidden states were predicted with castor (Louca and Doebeli, 2018) and pathways were inferred with MinPath (Ye and Doak, 2009). Predicted genes present in the studies microbial communities were classified into different metabolism's categories by mapping against MetaCyc database (Caspi et al., 2020; Kanehisa and Goto, 2000).

3 Results

3.1 Visual observations

245

The first evidence of the activity of the autochthonic/native microorganisms in the first month of the cultivation was the growth of the biofilm (Fig. 1). At the beginning of the cultivation, the fermentation solution was colourless. The colour started to change after three months of cultivation. The solutions became light yellow, which could be an effect of the dissolving of fulvic acids. After six months of cultivation, these microcosms contained a dark brown solution (Fig. 1), which changed to

250 almost black after 12 months. These observations indirectly suggest the dissolving of humic and fulvic acids and/or as biodegradation of OM by microbial communities/microorganisms from lignite-beds.

START OF INCUBATION	ANAEROBIC INCUBATION IN THE DARK AT THE TEMPERATURE 25°C				END OF INCUBATION
Field sampling	1 YEAR			2 YEARS	3 YEARS
October 2019	3 months	6 months	12 months		October 2022
Collection of raw detritic lignite samples from the opencast mine in Konin (Poland) Beginning of the experiment under oxygen-free atmosphere				NO ACTION / NO SHAKING ONLY STORAGE UPSIDE DOWN IN THE DARK WITHOUT INTERFERING THE INCUBATION	
OBSERVATIONS / TASKS	Biofilm growth in the fermentation liquid	Dissolving of fulvic acids and humic substance	Organic matter biodegradation **NO BIOGAS !**	---	Fermentation liquids are black **CO$_2$ PRODUCTION !**
• DNA extractions • GC-MS studies of OM • GC: CH$_4$ and CO$_2$ • TC and TN from medium • NO$_3^{2-}$ and NH$_4^+$ • pH and EC			• GC: CH$_4$ and CO$_2$ (4 samples)		• DNA extractions • GC-MS studies of OM • GC: CH$_4$ and CO$_2$ • TC and TN from medium • NO$_3^{2-}$ and NH$_4^+$ • pH and EC • δ^{13}C of CH$_4$ and CO$_2$

Figure 1: Time diagram of the research tasks and changes in the color of the fermentation liquid during anaerobic cultivation.

3.2 Biogas analyses

255 For the first testing (after 1 year) 4 samples were checked using GC methods and CH$_4$ as well CO$_2$ were not present in the headspace gas. The main component of the headspace at that time was N$_2$, the role of H$_2$ is unknown because we did not have the possibility of checking its concentration during cultivation. Headspace gases analysis after 3 years incubation revealed that the main gaseous product of lignite's decomposition was CO$_2$ (Table 2). Its concentration ranged from 14.5 to 25.6% (mean

concentration 20.7%). The trace component of the biogas was CH_4 whose concentration ranged from 11 to 49 ppm (mean

260   concentration 37 ppm). N_2O was not detected.

Table 2: Concentrations of gases (CH_4, CO_2), its $\delta^{13}C$ values and $\alpha^{13}C_{CO2-CH4}$ fractionation factor at the end of lignite cultivations.

Name	CH_4 [ppm]	SD	CO_2 [%]	SD	$\delta^{13}C(CH_4)$ [‰]	$\delta^{13}C(CO_2)$ [‰]	$\alpha^{13}C_{CO2-CH4}$
M9	37.2	1.0	16.1	9.1	-43.3	-21.4	1.023
M9A	36.9	4.3	25.2	0.1	-47.1	-22.7	1.026
M9B	45.2	3.1	24.8	0.7	-48.0	-23.7	1.026
M9C	48.8	4.5	14.5	8.5	-49.4	-25.1	1.026
M9D	34.6	6.4	18.1	1.3	-45.0	-15.4	1.031
M9E	17.4	1.7	24.7	0.3	-53.8	-25.0	1.030
MG	47.2	n.a.	15.2	5.2	-46.4	-20.3	1.027
MGA	39.8	5.0	21.9	4.9	-47.8	-23.7	1.025
MGB	40.6	4.9	17.5	11.4	-50.4	-25.8	1.026
MGC	44.4	3.0	25.6	2.0	-50.7	-24.9	1.027
MGD	40.1	5.6	20.7	5.4	-45.8	-12.5	1.035
MGE	11.5	1.3	24.0	0.4	-47.2	-14.5	1.034

The lowest concentration of CH_4 were determined for incubations with the additive of methanol (M9E and MGE). The high

concentrations of CH_4 were characterised by cultivations with nutrient broth and yeast extract – 48.8 ppm for M9C and 44.4

265   ppm for MGC. However, an unexpectedly high CH_4 concentration, 47.2 ppm, was observed in the experiment containing only

M9 medium (M9). All concentrations were much higher than atmospheric concentrations (1.8 ppm), which indicates the

biological origin of CH_4. The lowest concentrations of CO_2 were detected in cultivation with M9 medium (M9 and MG).

Relatively high CO_2 concentrations were characterized for cultivations with methanol and equalled 24.7% for M9E and 24.0%

for MGE. However, CO_2 concentrations in almost half of the cultivations indicate a high variability expressed by the SD index

270   above 5. The concentration of O_2 was checked to detect potential leakage or contamination with atmospheric air. In all analysed

headspace gas samples, no O_2 was detected.

The $\delta^{13}C(CH_4)$ values were in range from -53.8 to -43.3‰. The $\delta^{13}C(CO_2)$ values ranged from -25.1 to -12.5‰. The isotope

fractionation factor $\alpha^{13}C_{CO2-CH4}$ ranged from 1.023 to 1.0267 in most cultivations containing pure M9 media, or additives of

nutrient broth and yeast extract. Higher values above 1.03 were characterized for the cultivations containing sodium acetate

275 (M9D and MGD) and methanol (M9E and MGE).

3.3 Fermentation liquids analyses

The total carbon (TC) concentrations in the fermentation liquids at the beginning of the cultivation ranged from 0 to 1128.4

mg/L. After 3-year cultivation, these concentrations were in the range from 481.7 to 1686.6 mg/L. The highest total carbon

concentrations were observed in the cultivations including yeast extract, nutrient broth, and sodium acetate (M9D and MGD).

280 The highest decrease of TC was observed in cultivations containing only M9 medium (M9 and MG).

The pH of the liquids decreased slightly during the cultivation from 7.5 to 6.6 (or near 6.9-7.0 in cases of cultivation with

sodium acetate). The EC increased during the cultivation which resulted most probably from dissolving of HCO_3^- ions (balance

processes of CO_2 in the solutions) and dissolving of the compounds from the lignite (like inorganic mineral matter e.g.

sulphates or iron hydroxides). It is also worthy to note that M9 minimal media used in this work has EC value equalled 1250

285 µS/cm. A similar value of EC (1290 and 1295 µS/cm) was measured for the M9E and MGE cultivations with the addition of

methanol (Table 3).

Table 3: The TC, pH and EC values of fermentation liquids at the beginning and end of lignite cultivations.

	TC [mg/L]			pH		EC [µS/cm]	
Name	**T0 Start**	**T1 End**	**ΔTC T0-T1**	**T0 Start**	**T1 End**	**T0 Start**	**T1 End**
M9	0.0	965.0	-965.0	7.5	6.6	1250	7533
M9A	407.8	864.1	-456.3	7.5	6.6	1291	7251
M9B	290.1	969.8	-679.7	7.5	6.6	1315	7239
M9C	342.4	568.9	-226.5	7.5	6.6	1299	7609
M9D	1067.4	1217.7	-150.3	7.5	7.0	2858	7964
M9E	1128.4	481.7	**646.7**	7.5	6.7	1290	8789
MG	0.0	819.8	-819.8	7.5	6.7	1251	7483
MGA	407.8	649.4	-241.6	7.5	6.6	1293	7602
MGB	290.1	686.4	-396.3	7.5	6.6	1317	7091
MGC	342.4	1071.5	-729.1	7.5	6.6	1233	8031
MGD	1067.4	1686.6	-619.2	7.5	6.9	2860	7896

|							
MGE	1128.4	466.1	**662.3**	7.5	6.7	1295	8868

The total nitrogen (TN) content in the fermentation liquid ranged from 281.9 to 344.0 mg/L at the beginning of the cultivation and from 125.0 to 218.2 mg/L at the end of the cultivation (after 3 years) (Table 4). The highest TN concentrations were observed in the cultivation with yeast extract, nutrient broth, and methanol (M9E and MGE). Total inorganic nitrogen (TIN) content decreased in all the samples at the end of cultivation. The lowest TIN values were determined in cultivation with sodium acetate (M9D and MGD) in the range from 68.6 to 70.2 mg/L. The highest TIN values were in cultivation with methanol (M9E and MGE) in the range from 129.3 to 164.7 mg/L. The compound responsible for the high values of TN in the fermentation liquid was NH_4^+, originally present in the minimal media M9 (NH_4Cl concentration 1 g/L). The total organic nitrogen (TON) in samples at the beginning of the experiments originated from the additives – yeast extract and nutrient broth and ranged from 43.7 to 62.1 mg/L. In the samples at the end of cultivation, TON values were in the range from 23.0 to 91.5 mg/L and differed between the cultivations without any correlation (Table 4). Only the cultivation with minimal media M9 named M9 and MG indicates a clear increase of TON values from 0 to 34.3 and 23.0 mg/L respectively.

Table 4: The concentrations of different nitrogen forms (TN, TIN, TON, NO_3^-, NH_4^+) in liquids at the beginning and end of lignite cultivations.

	TN [mg/L]		TIN [mg/L]		NO_3^- [mg/L]		NH_4^+ [mg/L]		TON [mg/L]	
Name	T0 Start	T1 End	T0 Start	T1 End	T0 Start	T1 End	T0 Start	T1 End	T0 Start	T1 End
M9	281.9	141.6	281.9	107.3	0.0	1.8	337,2	111.8	**0.0**	**34.3**
M9A	344.0	137.9	281.9	87.9	0.0	7.4	337,2	85.3	62.1	50.0
M9B	325.5	134.0	281.9	97.2	0.0	9.4	337,2	96.7	43.7	36.8
M9C	338.3	164.6	281.9	107.6	0.0	6.2	337,2	110.9	**56.5**	**57.1**
M9D	338.3	147.1	281.9	70.2	0.0	0.0	337,2	64.7	**56.5**	**76.9**
M9E	338.3	210.6	281.9	129.3	0.0	1.6	337,2	140.2	**56.5**	**81.2**
MG	281.9	128.9	281.9	105.8	0.0	3.3	337,2	109.5	**0.0**	**23.0**
MGA	344.0	138.3	281.9	104.7	0.0	1.6	337,2	108.5	62.1	33.6
MGB	325.5	125.0	281.9	97.4	0.0	5.3	337,2	98.1	43.7	27.7
MGC	338.3	168.7	281.9	124.8	0.0	7.8	337,2	132.6	56.5	43.9
MGD	338.3	160.2	281.9	68.6	0.0	0.0	337,2	62.6	**56.5**	**91.5**
MGE	338.3	218.2	281.9	164.7	0.0	2.5	337,2	185.5	56.5	53.5

3.4 GC-MS analyses

he total extract of OM from detritic lignite indicates significant changes in their molecular composition (Fig. 2). These changes include both a decrease in compound concentrations and the appearance of new compounds that are products of the
305   decomposition of lignite and/or biomass.
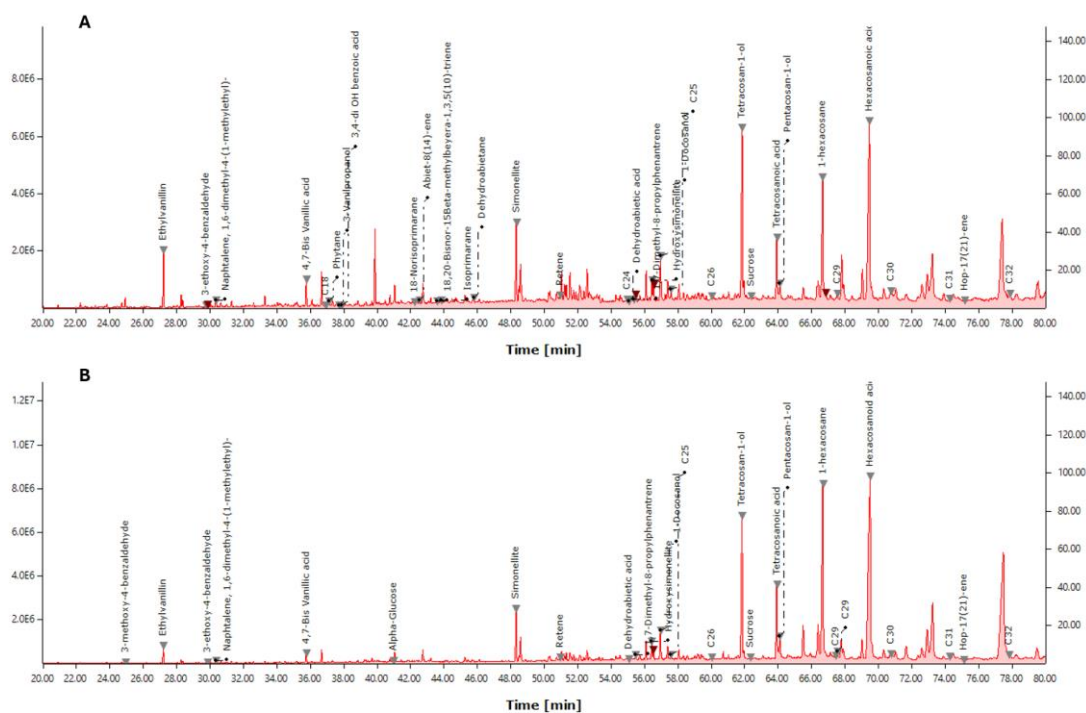
Figure 2: Total ion chromatogram of the detritic lignite at the beginning (A) and end of 3 year cultivation experiment (B).

The new compounds whose concentrations increased due to the biodegradation were: benzaldehyde; benzoic acid; α-glucose; 18-norisoprimarane; 18,20-bisnor-15β-methylbeyera-1,3,5(10)-triene; retene; ferruginol; dehydroabietic acid; 1,7-dimethyl-8-
310   propylphenantrene; hydroxysimonellite; 1-docosanol; tetracosan-1-ol; tetracosanoic acid; pentacosan-1-ol; 1-hexacosane; n-hexacosanoic acid; 1,27-heptacosanedioic acid.

The biodegraded compounds originally present in lignite OM and which concentrations in total extracts decreased after cultivation were: 3-ethoxy-4benzaldehyde; 3-ethoxy-4-benzaldehyde; naphthalene; 4,7-bis vanillic acid; phytane; 3-vanilpropanol; 3,4-di OH benzoic acid; abiet-8(14)-ene; isoprimarane; dehydroabietane; simonellite; 1,7-dimethyl-8-
315   propylphenantrene; sucrose; hop-17(21)-ene. Concentrations of n-alkanes (from n-C_{18} to n-C_{24}) decreased almost to zero,

15

whereas in case of n-C$_{29}$, n-C$_{30}$ and n-C$_{31}$ their concentrations increased due to biodegradation. The Table 5 showed the content

of all identified compounds from the total extracts.

Table 5: Molecular composition of lignite samples at the beginning and after cultivation (all data calculated from total ion chromatogram of total extracts).

	Lignite before cultivation	Lignite after cultivation				
Compound	Content in the total extract [ug/g of sample]					
New biodegradation products (concentrations increased)	W5	MG	MGC	MGD	MGE	Mean content
Benzaldehyde, 3-methoxy-TMS	0	0.0009	0.0014	0	0	0.0012
Benzoic acid TMS	0	0	0.0005	0	0	n.a.
α--Glucose-TMS	0.0008	0	0	0.0011	0.0007	0.0009
18-Norisoprimarane	0.0007	0	0.0014	0.0017	0	0.0015
18,20-Bisnor-15β-methylbeyera-1,3,5(10)-triene	0.0007	0	0.0016	0.0017	0	0.0016
Retene	0.0019	0.0029	0.0029	0.0042	0.0012	0.0028
Ferruginol	0	0	0.0002	0.0004	0	0.0003
Dehydroabietic acid-TMS	0.0003	0.0005	0.0008	0.0020	0.0021	0.0013
1,7-Dimethyl-8-propylphenantrene	0.0008	0	0.0014	0.0013	0	0.0013
Hydroxysimonellite	0.0203	0.0226	0.0254	0.0301	0.0165	0.0237
1-Docosanol, TMS	0.0493	0.0423	0.0622	0.0623	0	0.0556
Tetracosan-1-ol TMS	0.1964	0.2142	0.3967	0.3475	0.1765	0.2837
Tetracosanoic acid, TMS	0.0658	0.1029	0.1537	0.1315	0.0557	0.1109
Pentacosan-1-ol TMS	0.0207	0.0345	0.0448	0.0388	0.0180	0.0340
1-hexacosane TMS	0.1645	0.3540	0.4788	0.3706	0.1769	0.3451
Hexacosanoic acid, TMS	0.3229	0.5601	0.4597	0.7382	0.2935	0.5129
1,27-Heptacosanedioic acid - TMS	0	0.0584	0.0868	0.0350	0.0023	0.0456
Compounds degraded (concentrations decreased)						
3-ethoxy-4-benzaldehyde TMS	0.0025	0.0015	0.0025	0.0020	0	0.0020
Naphtalene, 1,6-dimethyl-4-(1-methylethyl)-	0.0062	0.0028	0.0047	0.0055	0.0017	0.0037
Vanillic acid TMS	0.0252	0.0113	0.0225	0.0207	0	0.0182
Phytane	0.0060	0	0	0	0	n.a.
3-Vanilpropanol, TMS	0.0008	0	0	0.0035	0	n.a.
3,4-di OH benzoic acid - TMS	0.0009	0	0	0	0	n.a.

|						
Abiet-8(14)-ene	0.0030	0	0	0.0017	0	n.a.
Isoprimarane	0.0024	0	0	0	0	n.a.
Dehydroabietane	0.0077	0	0	0	0	n.a.
Simonellite	0.0755	0.0658	0.0521	0.0623	0.0238	0.0510
1,7-Dimethyl-8-propylphenantrene	0.0080	0.0067	0.0055	0.0062	0.0027	0.0053
Sucrose-TMS	0.0051	0.0020	0.0037	0.0075	0.0019	0.0038
Hop-17(21)-ene	0.0015	0.0001	0	0	0	n.a.
***n*-Alkanes**						
C_{17}	0	0	0	0.0003	0	n.a.
C_{18}	0.0011	0	0	0	0	n.a.
C_{24}	0.0015	0	0.0015	0.0012	0.0006	0.0008
C_{25}	0.0097	0.0061	0.0083	0.0080	0.0062	0.0071
C_{26}	0.0049	0.0027	0.0051	0.0067	0.0031	0.0044
C_{27}	0	0	0.0001	0	0	n.a.
C_{29}	0.0100	0.0116	0.0148	0.0139	0.0057	0.0115
C_{30}	0.0182	0.0089	0.0177	0.0165	0.0130	0.0140
C_{31}	0.0031	0.0050	0.0086	0.0076	0.0038	0.0063
C_{32}	0.0153	0.0003	0	0	0.0097	n.a.
n.a. – not analysed						

3.5 Microbiological analyses

Microbiome structure analysis based on 16S rDNA sequencing showed a decrease in diversity in all cultivated samples where autochthonous microflora was stimulated, compared to the raw lignite (Tab. A1, Tab. A2, Fig 3). Pronounced changes in the microbiome composition were observed between samples (Fig. 3, Fig 4 and Fig. S1). There was decrease in detectable family's number from 123 for lignite sample to 60 in MG and 30, 26 and 25 for MGC, MGD and MGE respectively (Fig. 3). In the lignite 74 unique families were detected, while MG sample had 24 unique families. Only 11 families where present in each sample type and less than 10 families were detected in different samples or were unique for rest of the culture conditions (Fig. 3). However, in culture samples were detected families that was not detected in lignite (Fig. A1).
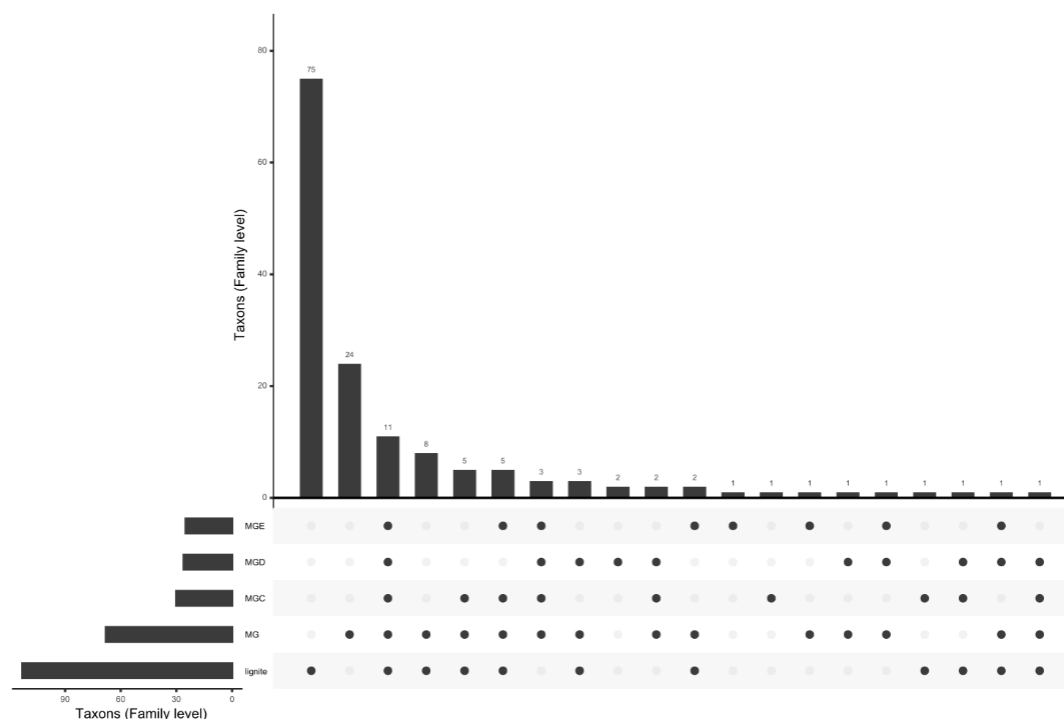
Figure 3: Upset plot showing the number of families shared between different samples and overall number of families per sample.
330   **Black dots indicate samples in which corresponding families have been detected.**

In all cultures abundance of *Micrococaceae* was increased in comparison to lignite, and in case of samples MG and MGC this

was the most enriched family relative to lignite, with 14.59 % and 38.24 % increase respectively (Fig. 4). For MGD members

of family *Dermathophilaceae* increased the most (24.11 %), and for MGE *Methylophilacea*_502230 family increased the most

(27.11 %), while other *Methylophilaceae* decreased in abundance in all sample for average of 5.42 %. The most abundant

335   family in lignite samples, *Gallionellaceae* completely diminished from the culture samples (Fig. 4). The second highest

decrease occurred for collective group of less dominant taxa ('other'on Fig. 4) except sample MGE where it was for
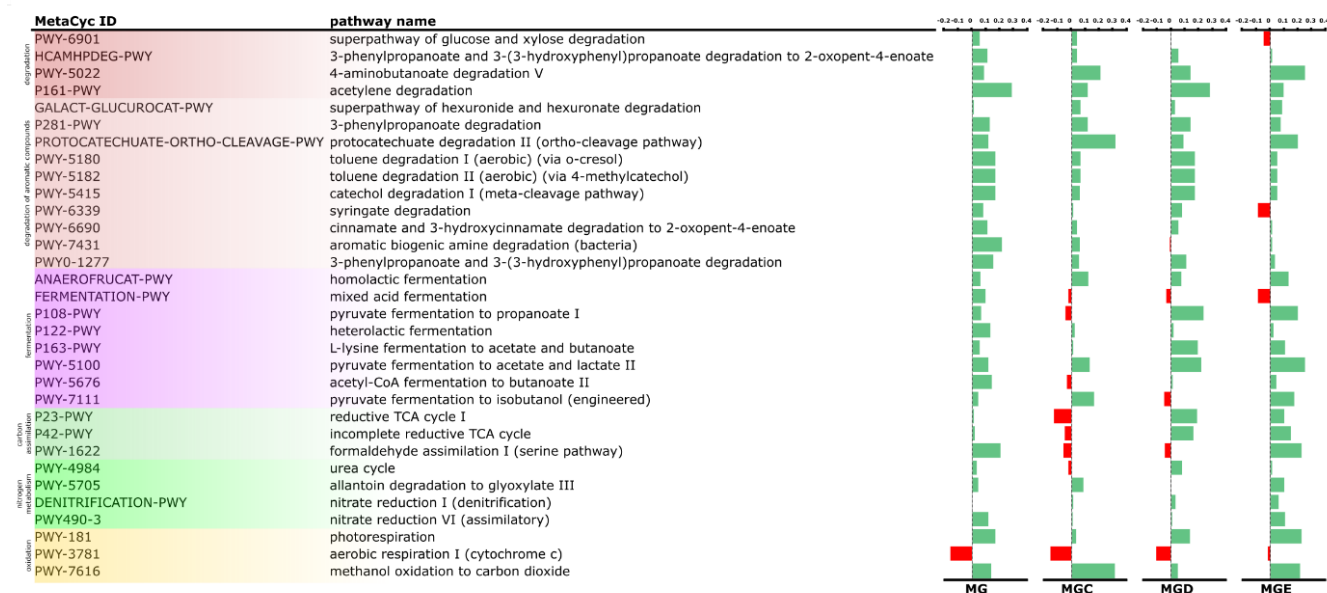
*Burkholderiaceae*_A_59252.
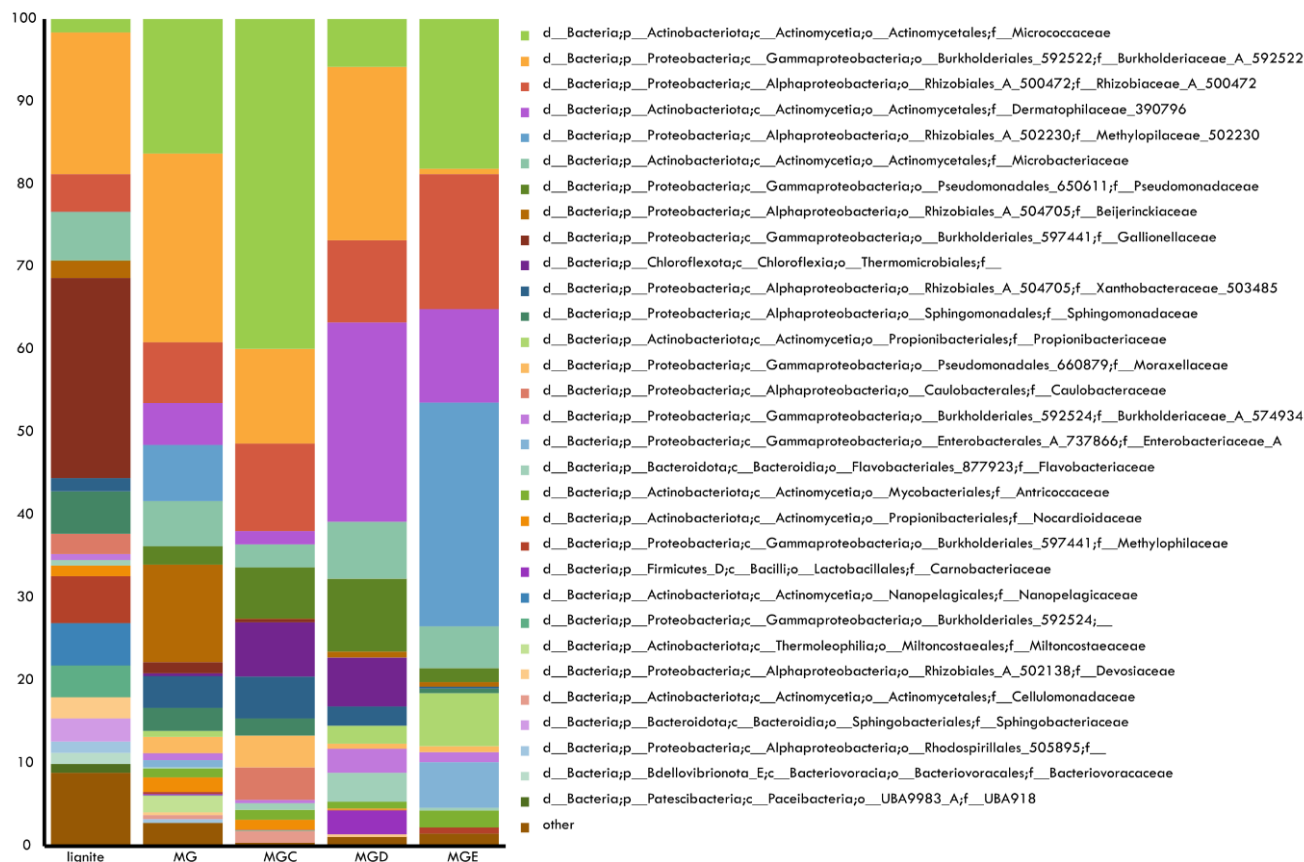
Figure 4: Microbial communities' structure in lignite and culture samples at the family level. Families that had abundance below 1% across all the samples were merged into a single group 'other'. For the lignite sample, the mean value of three repeats is shown.

The microbial communities in the cultured samples (MG1, MGC1, MGD1, MGE1) exhibit enrichment in nitrogen-cycling bacteria compared to the original lignite sample, with a clear increase of nitrogen cycling bacteria in the cultured samples compared to the lignite sample. In particular, *Rhizobiales* (involved in nitrogen fixation) (Deb et al., 2024) and *Burkholderiales* (involved in both N2-fixation and denitrification) (Berkelmann et al., 2020) are significantly enriched in MG1 and MGD1, while denitrifying bacteria *Sphingomonadaceae* (Dai et al., 2022) and *Pseudomonadaceae* are more abundant in MGC1 and MGE1.

Based on the microbiome structure functional predictions have been performed. Data for the relative abundance of pathways involved in the degradation of OM, nitrogen and sulphur metabolism based on the MetaCyc classification are presented on the Figure S1 in section Appendix A - Supplementary Material. Overall, 399 pathways have been predicted to be present in the

19

350 sample. Among pathways that were predicted to increase in culture where these connected with OM degradation, including

degradation of aromatic compounds as well as with fermentation. Predicted abundance of almost all pathways for carbon

assimilation were reduced in MGC samples while reductive TCA cycles were predicted to be increased in MGD and MGE

samples. From oxidative pathways, methanol oxidation to CO_2 was predicted to be increased in all culture sample (Fig. 5).

Figure 5: Prediction of pathways' abundance in the culture samples relative to the lignite samples. Bars indicate the increase (green) or decrease (red) in pathway abundance in the culture samples compared to lignite (relative in sample >0.1%).

For nitrogen cycling the denitrification pathway (DENITRIFICATION-PWY) was predicted to be more prominent in MGC

and MGE samples (Fig. 5). In contrast nitrogen-fixation (PWY-7084) was predicted to be more prevalent in MG and MGD

360 samples, while assimilatory nitrate reduction pathway (PWY-490-3) was predicted to be increased relative to lignite in all

cultures, although with different degree (Fig. 5).

4 Discussion

Biodegradation of immature sedimentary OM is well studied in context of microbial CH_4 formation. The reason this topic is

important and attractive to the scientific community is the potential applications of new knowledge in the industry. Many

365   lignite cultivation experiments are carried out using native microorganisms that has been previously cultivated and enriched,

for example, by growing methanogens. Coal material is also often pretreated by physical or chemical methods to obtain higher

CH_4 or biogas yield. Although laboratory techniques can ensure very fast and effective lignite substrate utilization, these

processes are selective, and they do not reflect natural conditions.

In this work we decided to use native microorganisms which were present in raw lignite samples and to check results of

370   microbial activity during 3-year experimental period. Any kind of cultivation would influence the structure of microbial

community by enrichment of some microorganisms while deterioration of others depending on the culture conditions and

medium composition used. For that reason, several media with different additives have been investigated in our study. As

expected, we saw the decrease in bacterial community diversity in the cultivation conditions. Nevertheless, some of the taxa

where present in all cultivations, while other where enriched based on the conditions. More importantly, functional prediction

375   suggested that although only a small number of families were common to all cultures, functionally communities showed some

similarities. Particularly, taxa with ability to degrade lignite derived OM have been enriched which is in accordance with

geochemical data presented here. The same was reflected in functional prediction analysis. However, it is important to

remember that this was prediction and in future studies of transcriptome or expression of selected genes a better picture of the

metabolic processes present in the cultivations can be provided. However, even between experiments that differ significantly

380   (e.g. addition of methanol or sodium acetate), common similarities can be observed in the processes, such as the degradation

of aromatic compounds, nutrient cycling, greenhouse gas emissions, and biomass growth, which reflect natural decomposition

pathways. Degradation of organic matter by biological agents is dependent on its availability to organisms, which is very

limited in the lignite deposits (Nelson et al., 1992). Nitrogen cycle is one of the crucial processes that influence decomposition

of lignite or organic matter in general (Stankiewicz and Van Bergen, 1998). In natural habitats, decomposition processes are

385   very slow when the C:N ratio of organic matter is above 30. In lignite habitats, this ratio is often many times higher. For

example, in the case of lignites from Konin the C:N ratio is between 120-150. This indicates that a nitrogen source is necessary

for optimal decomposition conditions. In our experiments, the main nitrogen source, easily available for the microorganisms

was NH_4Cl in the minimal media M9 (concentration of 1 g/L). The minor source was organic nitrogen present in the nutrient

broth or yeast extract. The main source of inorganic nitrogen was N_2 present in the headspace gas (85%), as the main

21

390   component of an oxygen-free atmosphere necessary for maintaining anoxic conditions. At the experimental conditions, we observed very slow dissolving of the fulvic, which occurred during 1st to 3rd month of the cultivation. The dissolving of fulvic acids does not need any microbial processes. These acids are the natural compounds in the lignite organic matter, and when the sample of lignite is raw, not crushed, can very slowly be dissolved in the fermentation liquid, which results in its yellow colour (Czechowski and Jezierski, 1997). Biodegradation of OM, especially lignite macromolecule (lignocelluloses or lignin),

395   requires microbial activity to break down the aromatic structure of lignin or lignin-maturation products (Bucha et al., 2020; Detman et al., 2018; Killops and Killops, 2005). These processes in the case of our experiments most probably started between the 3rd and 6th month of cultivation, which was reflected by changing the colour of the solution into brown or dark brown. After 1 year all the cultivated samples were characterised by the dark brown or even black colour of the fermentation liquid. Therefore, we can be sure that OM was undergoing degradation.

400   The decomposition of OM during the 1st year of cultivation did not result in the formation of large quantities of biogas. After the 3rd year of the cultivation the headspace gas samples were rich in CO_2. CH_4 was detected in samples after 3th year of cultivation, but rather as a trace gas (with a concentration around 50 ppm). The presence of CO_2 in the headspace gas in the range from 16 to 25% indicates that this was the main, final decomposition product. The CO_2 was also present in the solution, which resulted in increasing the EC – from HCO_{3-} ions. Stable isotope analysis of CH_4 and CO_2 suggested that in the case of

405   our experiments, the CH_4 oxidization was the main CH_4 sink and the dominant CO_2 forming process (Fig. 6).
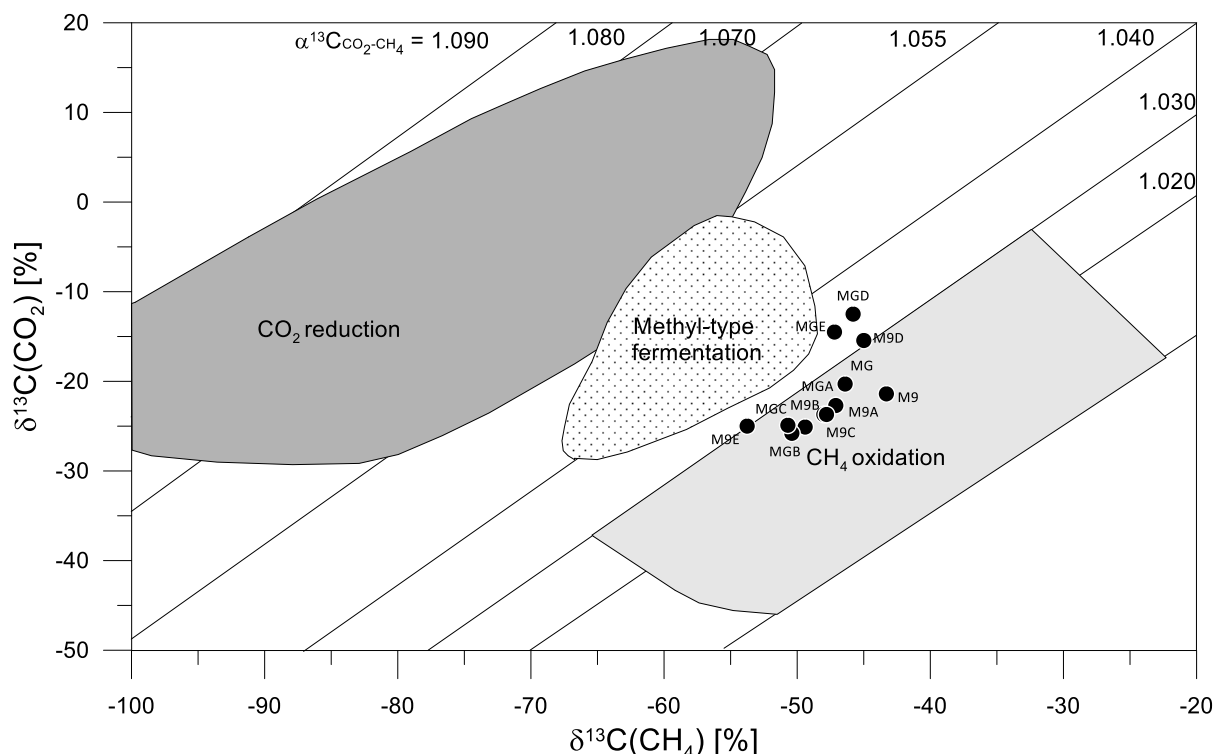
Figure 6: The isotopic composition of biogas (CH₄ and CO₂) after 3-year cultivation of lignite from Konin.

The GC-MS study of lignite OM revealed typical products of biodegradation, which are direct proof of lignocellulose communities' activity. The decomposition of OM from lignite usually is reflected by an increase in the amount of the aromatic compounds in the total extract (in our cultivations e.g. benzaldehyde; 18-norisoprimarane; retene; ferruginol) as well as organic acids (see Table 5). Appearance of new aromatic compounds is associated a simultaneous decrease in the amount of the *n*-alkanes (Fabiańska, 2007; Bucha et al., 2018; Detman et al., 2018). The role of sugars is also very important because they are naturally occurring in lignite deposits, especially in fossil wood. Fossil wood fragments are often dispersed in detritic lignite, which results in the presence of sugar in the total extract of detritic coal (Marynowski et al., 2018). Therefore, sucrose was originally the sugar present in our lignite and was an easily available, minor source of energy for microorganisms. Generally, carbon metabolism in the case of our cultivations plays a main role which results in the formation of CO_2, oxidation of CH_4, dissolving of fulvic and humic acids due to natural processes and biodegradation. We observed that the degradation of coal produces organic acids (e.g. benzoic acid; dehydroabietic acid; tetracosanoic acid; hexacosanoic acid; 1,27-heptacosanedioic acid). This process was reflected by decreasing of pH of the solution from 7.5 to around 6.5 (in most cases). The dynamics of

420 changes in CH_4 and CO_2 concentrations during the course of experiment or TC of the solution at different incubation time

points are among issues that await elucidation and need to be addressed in future studies.

The GC-MS analyses were supported by functional prediction analysis of bacteriobiome, which revealed presence of metabolic

pathways related to organic compounds present in lignite decomposition products. The potential processes associated with the

biodegradation products, as determined through geochemical investigation, included pyruvate fermentation to isobutanol,

425 pyruvate fermentation to propionate, homolactic fermentation, protocatechuate degradation (protocatechuic acid, also known

as dihydroxybenzoic acid, is present in the organic matter extracts after degradation), glucose and xylose degradation, and urea

cycling (NH_4^+ cycling from the M9 minimal medium).

The nitrogen cycling in experiments was also relevant. Based on geochemical results we determined significant changes in

TN, TIN and TON values at the start and end of the cultivation. The main compound that affected the TN values was NH_4^+

430 ion (which was expressed by $R^2=0.50$, Fig. 7).
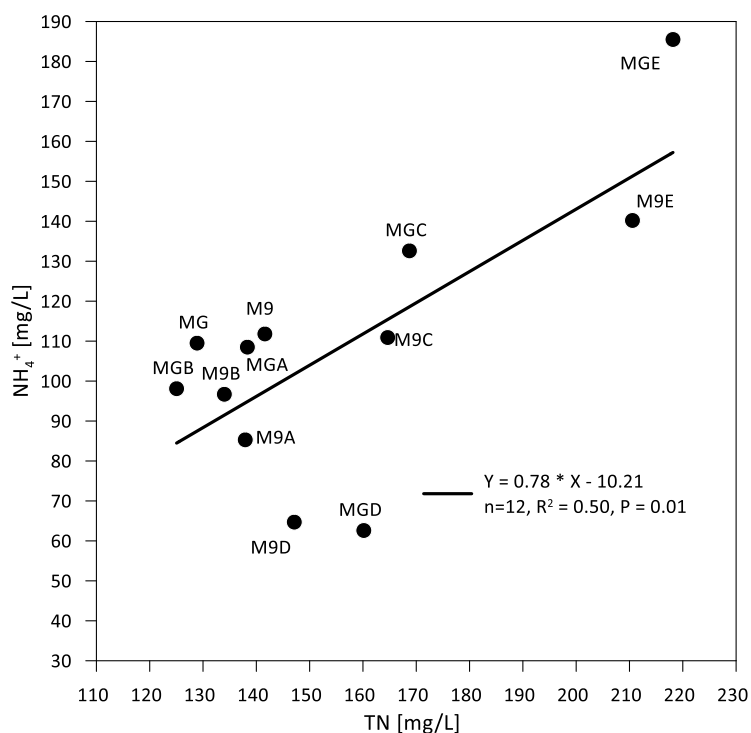
Figure 7: Relation between TN values and NH_4^+ concentrations at the end of cultivation.

The availability of NH_4^+ seems to be crucial for all cultivations because the lignite OM is lacking in nitrogen. The typical values of TN in coals from Konin are between 0.2-0.6% by weight (Bucha et al., 2020). Moreover, these coals are still under

435 the stadium of diagenesis and microbial decomposition (Fabiańska and Kurkiewicz, 2013), therefore it can be predicted that in the future (in geological age scale), the amount of available nitrogen from these organic-rich sediments will decrease. The deposits are outcropped, so the rainfall of weathering conditions (as oxidizing of sulphides) occurs naturally (Chang and Berner, 1999; Fabiańska et al., 2024). This can transfer some of the N_2-fixing microorganisms into the layers of coal as well as mineral nutrients together with rainfall water (Pytlak et al., 2020). It is also worth noting that the deposit has contact with

440 atmospheric air, which is the largest pool of inorganic nitrogen on Earth (Deb et al., 2024; Lewicka-Szczebak et al., 2021; Müller and Clough, 2014).

Analyses of fermentation liquids showed that the inorganic form of nitrogen dominated over organic. Nitrogen is used by bacteria for growth, most of the biomass cells should be attached to the coal surface and not present or dispersed in the solution. The balance of nitrogen cannot be closed, because of missing crucible information regarding the amount of N_2 dissolved in

445 the solution. For our calculation, we assumed (based on the literature data) that the theoretical maximal amount of N_2 dissolved in water at 20°C is 20 mg/L. Therefore, TON from the fermentation liquid can contain organic compounds from lignin degradation in amounts of 27.7 to 91.5 mg/L. However, the lignin degradation products are humic acids, which could not be detected in extract and GC-MS because of their large molecule size

The decomposition of lignite OM, which took place during cultivations was probably connected with N_2 fixation at anaerobic

450 conditions. Under anaerobic conditions, NH_4^+ can be directly converted to organic nitrogen by many organisms and plants. Nitrogen assimilation is connected with anaerobic CH_4 oxidation, but this process is not yet sufficiently studied (Larmoia et al., 2014). Recent studies (Hara et al., 2022; Minamisawa et al., 2016) showed that in anoxic environments of rice paddy soils or with the presence of aromatic compounds the anaerobic N_2-fixation plays an important role in the processes of decomposition. Unfortunately, for the lignite or other coal-rich environments, this knowledge is still very unique and not

455 widely known. We hypothesise, that N_2-fixation processes at surface or subsurface processes in lignite deposits are very common. First of all, our bacteria community analysis clearly showed enrichment of the N_2-fixing microorganisms in our cultivations in comparison to lignite. Many of them are also responsible for degradation of organic compounds.

Three main families of *Rhizobiales* present in our samples were *Beijerinckiaceae*, *Rhizobiaceae*, and *Methylopilaceae*. Members of the family *Beijerinckiaceae* include chemoorganoheterotrophs, facultative methylotrophs, facultative methanotrophs, and obligate methanotrophs (Rosenberg et al., 2014). The ability to utilize multicarbon compounds (with more than one carbon in the molecule) is variable but is generally broader in chemoorganoheterotrophs, followed by facultative methylotrophs, and then facultative methanotrophs (Rosenberg et al., 2014; Tamas et al., 2010; Yurimoto et al., 2021). They can grow in a wide range of pH (including values as low as 3.0 units) and are known to show a preference for sugars as carbon sources. Members of the genus *Beijerinckia* are commonly found as free-living bacteria in acidic soils and also in plant rhizosphere and phyllosphere environments (Tamas et al., 2010). *Beijerinckia* can degrade polycyclic aromatic hydrocarbons such as anthracene, biphenyl, dibenzofuran, and phenanthrene, among others (Kiyohara al., 1983). The family of the *Rhizobiaceae* uses a large variety of carbohydrates and salts from organic acids as their carbon source and uses ammonium salts, nitrate, and several amino acids as their nitrogen source. These bacteria are not able to perform carbon assimilation. *Methylopilaceae* are methanotrophs, with the ability to grow using methanol. The species *Methylopila oligotropha* was found in soil from a Russian salt mine and described as tolerant to salt stress (Beck et al., 2015; Dedysh et al., 2005).

Nitrogen cycling bacterial taxa have been detected in all samples (Fig. 8), although there were enriched in the cultures which might be associated with N_2-atmosphere used in the study. Among the most enriched families involved in nitrogen cycling were *Rhizobiales*, *Burkholderiales*, *Pseudomonadaceae*, and *Sphingomonadaceae* which reflects their roles in either nitrogen fixation or denitrification and emphasize how experimental conditions have facilitated the growth of microbial communities capable of nitrogen cycling.

taxonomy	lignite	MG	MGC	MGD	MGE
d__Bacteria;p__Actinobacteriota;c__Actinomycetia;o__Actinomycetales;f__Micrococcaceae	●	●	●	●	●
d__Bacteria;p__Proteobacteria;c__Gammaproteobacteria;o__Burkholderiales_592522;f__Burkholderiaceae_A_592522	●	●	●	●	●
d__Bacteria;p__Proteobacteria;c__Alphaproteobacteria;o__Rhizobiales_A_500472;f__Rhizobiaceae_A_500472	●	●	●	●	●
d__Bacteria;p__Actinobacteriota;c__Actinomycetia;o__Actinomycetales;f__Dermatophilaceae_390796	○	●	●	●	●
d__Bacteria;p__Proteobacteria;c__Alphaproteobacteria;o__Rhizobiales_A_502230;f__Methylopilaceae_502230	●	●	○	○	●
d__Bacteria;p__Actinobacteriota;c__Actinomycetia;o__Actinomycetales;f__Microbacteriaceae	●	●	●	●	●
d__Bacteria;p__Proteobacteria;c__Gammaproteobacteria;o__Pseudomonadales_650611;f__Pseudomonadaceae	●	●	●	●	●
d__Bacteria;p__Proteobacteria;c__Alphaproteobacteria;o__Rhizobiales_A_504705;f__Beijerinckiaceae	●	●	●	●	●
d__Bacteria;p__Proteobacteria;c__Gammaproteobacteria;o__Burkholderiales_597441;f__Gallionellaceae	●	●	●	○	○
d__Bacteria;p__Chloroflexota;c__Chloroflexia;o__Thermomicrobiales;f__	○	●	●	●	○
d__Bacteria;p__Proteobacteria;c__Alphaproteobacteria;o__Rhizobiales_A_504705;f__Xanthobacteraceae_503485	●	●	●	●	●
d__Bacteria;p__Proteobacteria;c__Alphaproteobacteria;o__Sphingomonadales;f__Sphingomonadaceae	●	●	●	○	●
d__Bacteria;p__Actinobacteriota;c__Actinomycetia;o__Propionibacteriales;f__Propionibacteriaceae	○	●	○	●	●
d__Bacteria;p__Proteobacteria;c__Gammaproteobacteria;o__Pseudomonadales_660879;f__Moraxellaceae	○	●	●	●	●
d__Bacteria;p__Proteobacteria;c__Alphaproteobacteria;o__Caulobacterales;f__Caulobacteraceae	●	●	●	○	○
d__Bacteria;p__Proteobacteria;c__Gammaproteobacteria;o__Burkholderiales_592524;f__Burkholderiaceae_A_574934	●	●	●	●	●
d__Bacteria;p__Proteobacteria;c__Gammaproteobacteria;o__Enterobacterales_A_737866;f__Enterobacteriaceae_A	○	●	○	○	●
d__Bacteria;p__Bacteroidota;c__Bacteroidia;o__Flavobacteriales_877923;f__Flavobacteriaceae	●	●	●	●	●
d__Bacteria;p__Actinobacteriota;c__Actinomycetia;o__Mycobacteriales;f__Antricoccaceae	○	●	●	●	●
d__Bacteria;p__Actinobacteriota;c__Actinomycetia;o__Propionibacteriales;f__Nocardioidaceae	●	●	●	●	●
d__Bacteria;p__Proteobacteria;c__Gammaproteobacteria;o__Burkholderiales_597441;f__Methylophilaceae	●	●	●	●	●
d__Bacteria;p__Firmicutes_D;c__Bacilli;o__Lactobacillales;f__Carnobacteriaceae	○	●	○	●	○
d__Bacteria;p__Actinobacteriota;c__Actinomycetia;o__Nanopelagicales;f__Nanopelagicaceae	●	○	○	○	○
d__Bacteria;p__Proteobacteria;c__Gammaproteobacteria;o__Burkholderiales_592524;__	●	●	●	○	○
d__Bacteria;p__Actinobacteriota;c__Thermoleophilia;o__Miltoncostaeales;f__Miltoncostaeaceae	○	●	○	○	○
d__Bacteria;p__Proteobacteria;c__Alphaproteobacteria;o__Rhizobiales_A_502138;f__Devosiaceae	●	●	○	●	○
d__Bacteria;p__Actinobacteriota;c__Actinomycetia;o__Actinomycetales;f__Cellulomonadaceae	○	●	●	●	○
d__Bacteria;p__Bacteroidota;c__Bacteroidia;o__Sphingobacteriales;f__Sphingobacteriaceae	●	●	●	○	●
d__Bacteria;p__Proteobacteria;c__Alphaproteobacteria;o__Rhodospirillales_505895;f__	●	●	○	●	○
d__Bacteria;p__Bdellovibrionota_E;c__Bacteriovoracia;o__Bacteriovoracales;f__Bacteriovoracaceae	●	○	○	○	○
d__Bacteria;p__Patescibacteria;c__Paceibacteria;o__UBA9983_A;f__UBA918	●	○	○	○	○

Figure 8: Dot plot showing the detection of specific families in particular samples. Black dots indicate the presence of the family, white dots indicate no detection of the family. Families which at least in one sample showed relative abundance >1% are included.

In summary, MG1 and MGD1 are dominated by N_2-fixation activities, with enrichment of *Rhizobiales* and *Burkholderiales*, while MGC1 and MGE1 show enhanced denitrification potential, with the increased presence of *Pseudomonadaceae* and *Sphingomonadaceae*. The selective enrichment of specific microbial taxa underscores the potential for dynamic nitrogen cycling. However, further studies are needed to fully comprehend the mechanisms driving these processes and their implications for nitrogen cycling in natural coal ecosystems.

Our previous studies also showed the presence of *Rhizobiales* in DNA isolated from experiments with detritic coals (Bucha et al., 2020). The results of bacterial communities from current experiments showed that N_2-fixing bacteria potentially can play a very important role in the coal/lignite microbiomes. We assume that nitrogen from the mineral medium was incorporated by microorganisms during biomass growth. The organic form of nitrogen can also originate from the lignin degradation

compounds (Fioretto et al., 2005). The headspace atmosphere contained N_2 which can be fixed by some microorganisms also under anaerobic conditions (Dey et al., 2021). During anaerobic cultivations, N_2O can be produced (Deb et al., 2024), but till now has not been detected in coal cultivations. Some researchers (Finzi et al., 2007; Van Groenigen et al., 2015; Zak et al., 2003) revealed unknown mechanisms of N_2-fixation at high levels of atmospheric CO_2. Additional microbiological and geochemical experiments are needed to unequivocally confirm the N_2-fixation processes. A crucial aspect of deepening our knowledge of the nitrogen cycle and N_2O sources is the distinction between nitrogen pools available as labile and non-labile OM (Lewicka-Szczebak et al., 2021; Müller et al., 2014). Therefore, it is very important to observe changes in the geochemical composition of the OM and tracing of carbon and nitrogen during microbial processes. The determination of C:N ratio changes, as well as $\delta^{13}C$ and $\delta^{15}N$ values in OM, help to quantify carbon and nitrogen budget during early and late diagenesis and will allow for better tracing of natural emissions of "greenhouse gases". This also can help to increase the knowledge regarding global carbon and nitrogen cycling and find effective mitigation strategies, especially in agricultural practices (Zaman et al., 2021).

5 Conclusions

Our study showed that under anaerobic conditions the natural microbial communities present in lignite from open pit are active and cause significant changes to OM molecular composition. The degradation of the lignite polymer was manifested by changes in liquid colour to the dark brown or black solution within one year. Microbial activity was supported by the production of CO_2 and its release to the headspace. Interestingly, no significant amounts of methane were detected in the headspace. Its concentrations were most often below 50 ppm. The results of stable isotope analyses of CH_4 and CO_2 indicate possible CH_4 oxidation processes. The dominant degradation process was lignin decomposition. Geochemical analysis revealed that the concentration of several aromatic compounds was increased due to OM decomposition, however new products were also determined to be present in the OM extracts. Analysis of bacterial structure showed that *Rhizobiales* were one of the most abundant orders in the communities from the analysed cultures. The role of nitrogen cycling in lignite deposits remains still not explained, but our results are in accordance with previous studies and confirm the increasing amount of *Rhizobiales* in all analysed samples during lignite incubation. Explanation of nitrogen cycling in coal habitats requires further studies (e.g. gene expression studies, cultivation for specific conditions). Prediction of microbial community metabolic activity is in accordance with other results showing lignite degradation. The important processes during lignite decomposition were also determined and confirmed by geochemical investigation. These are pyruvate fermentation to propionate, homolactic fermentation, protocatechuate degradation, glucose and xylose degradation, and urea cycle. The majority of predicted fermentation pathways

present in the communities also increased in abundance in culture conditions. This prediction correlates with observed lignite biotransformation products and supports the degradation of OM from lignites. More research is needed to be certain which pathways are, in fact active in the communities during lignite biotransformation. This important topic should be further investigated in the future.
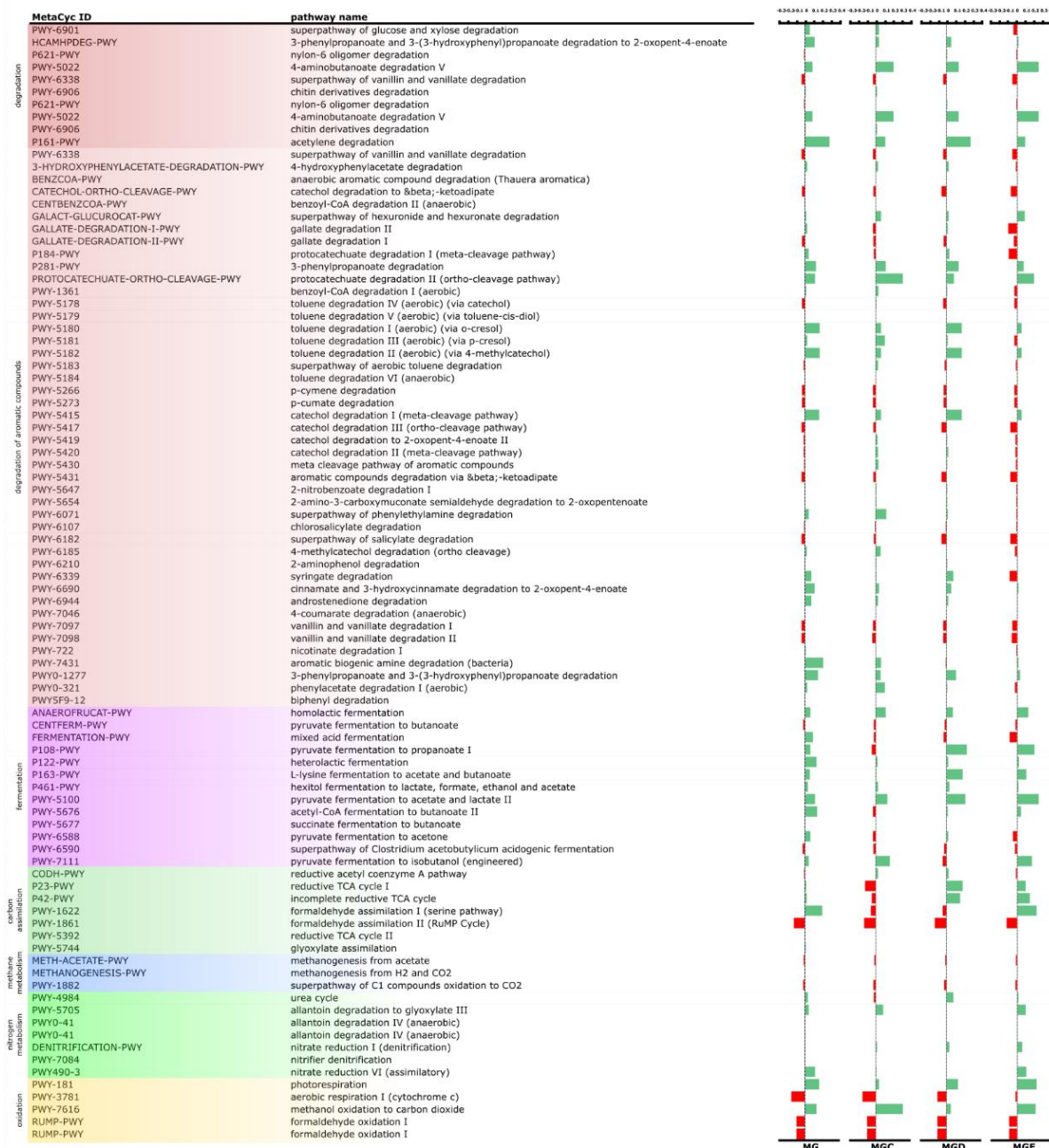
520 **Appendix A**

Figure A1: Prediction of pathways' abundance in the culture samples relative to the lignite samples. Bars indicate the increase (green) or decrease (red) in pathway abundance in the culture samples compared to lignite.

Table A1: Number of reads in lignite and incubation samples obtained using Picrust software.

Category	Pathway	Description	Number of reads				
			lignite	MG	MGC	MGD	MGE
Degradation	PWY-6901	superpathway of glucose and xylose degradation	30396	74984	68719	50532	31815
	HCAMHPDEG-PWY	3-phenylpropanoate and 3-(3-hydroxyphenyl)propanoate degradation to 2-oxopent-4-enoate	224	24654	7612	9508	1953
	P621-PWY	nylon-6 oligomer degradation	808	789	2014	2185	30
	PWY-5022	4-aminobutanoate degradation V	20295	60152	84654	57874	57032
	PWY-6338	superpathway of vanillin and vanillate degradation	6460	6074	6126	4454	1060
	PWY-6906	chitin derivatives degradation	0	1227	2486	30	0
	PWY0-41	allantoin degradation IV (anaerobic)	230	335	0	0	0
	P621-PWY	nylon-6 oligomer degradation	808	789	2014	2185	30
	PWY-5022	4-aminobutanoate degradation V	20295	60152	84654	57874	57032
	PWY-6338	superpathway of vanillin and vanillate degradation	6460	6074	6126	4454	1060
	PWY-6906	chitin derivatives degradation	0	1227	2486	30	0
	PWY0-41	allantoin degradation IV (anaerobic)	230	335	0	0	0
	P161-PWY	acetylene degradation	5090	72509	33978	56949	18244
	3-HYDROXYPHENYLACETATE-DEGRADATION-PWY	4-hydroxyphenylacetate degradation	3782	13227	12422	10487	3336
	BENZCOA-PWY	anaerobic aromatic compound degradation (Thauera aromatica)	24	0	0	0	0
	CATECHOL-ORTHO-CLEAVAGE-PWY	catechol degradation to β-ketoadipate	10273	14212	15062	7895	3181
	CENTBENZCOA-PWY	benzoyl-CoA degradation II (anaerobic)	17	0	0	0	0
	GALACT-GLUCUROCAT-PWY	superpathway of hexuronide and hexuronate degradation	9408	22215	32480	19802	22450
	GALLATE-DEGRADATION-I-PWY	gallate degradation II	12009	30087	17847	21709	1140
	GALLATE-DEGRADATION-II-PWY	gallate degradation I	4500	3325	3669	2443	911
degradation of aromatic compounds	P184-PWY	protocatechuate degradation I (meta-cleavage pathway)	11253	32648	19037	24113	1254

31

P281-PWY	3-phenylpropanoate degradation	15271	59366	54946	49358	28441
PROTOCATECHUATE-ORTHO-CLEAVAGE-PWY	protocatechuate degradation II (ortho-cleavage pathway)	25943	79314	119518	57865	57505
PWY-1361	benzoyl-CoA degradation I (aerobic)	3525	10619	13077	6372	698
PWY-5178	toluene degradation IV (aerobic) (via catechol)	4002	1687	9788	89	1329
PWY-5179	toluene degradation V (aerobic) (via toluene-cis-diol)	157	0	0	0	0
PWY-5180	toluene degradation I (aerobic) (via o-cresol)	4654	46273	22101	37677	11982
PWY-5181	toluene degradation III (aerobic) (via p-cresol)	6219	17724	33939	11825	3897
PWY-5182	toluene degradation II (aerobic) (via 4-methylcatechol)	4654	46273	22101	37677	11982
PWY-5183	superpathway of aerobic toluene degradation	2009	1136	9605	0	1128
PWY-5184	toluene degradation VI (anaerobic)	25	0	0	0	0
PWY-5266	p-cymene degradation	3203	0	0	0	0
PWY-5273	p-cumate degradation	3203	0	0	0	0
PWY-5415	catechol degradation I (meta-cleavage pathway)	3857	43773	20310	36189	11141
PWY-5417	catechol degradation III (ortho-cleavage pathway)	10587	14039	16642	8362	3141
PWY-5419	catechol degradation to 2-oxopent-4-enoate II	1729	1460	7406	4269	59
PWY-5420	catechol degradation II (meta-cleavage pathway)	2203	2487	9755	6806	103
PWY-5430	meta cleavage pathway of aromatic compounds	1133	701	8679	3307	140
PWY-5431	aromatic compounds degradation via β-ketoadipate	10587	14039	16642	8362	3141
PWY-5647	2-nitrobenzoate degradation I	378	297	1542	1903	29
PWY-5654	2-amino-3-carboxymuconate semialdehyde degradation to 2-oxopentenoate	440	358	2135	1707	24
PWY-6071	superpathway of phenylethylamine degradation	4526	18225	35195	9977	4803
PWY-6107	chlorosalicylate degradation	824	468	0	0	500
PWY-6182	superpathway of salicylate degradation	11185	15965	18780	9440	3618
PWY-6185	4-methylcatechol degradation (ortho cleavage)	3991	11657	19135	7016	2090

	PWY-6210	2-aminophenol degradation	203	217	1286	1228	17
	PWY-6339	syringate degradation	10519	38372	23088	30835	1798
	PWY-6690	cinnamate and 3-hydroxycinnamate degradation to 2-oxopent-4-enoate	224	24654	7612	9508	1953
	PWY-6944	androstenedione degradation	413	17166	6202	3355	224
	PWY-7046	4-coumarate degradation (anaerobic)	266	0	24	0	0
	PWY-7097	vanillin and vanillate degradation I	6460	6074	6126	4454	1060
	PWY-7098	vanillin and vanillate degradation II	7120	6791	6803	4965	1183
	PWY-722	nicotinate degradation I	900	2944	1975	1828	159
	PWY-7431	aromatic biogenic amine degradation (bacteria)	7665	62454	27848	11584	10885
	PWY0-1277	3-phenylpropanoate and 3-(3-hydroxyphenyl)propanoate degradation	749	34314	12952	20343	4771
	PWY0-321	phenylacetate degradation I (aerobic)	5685	17713	33075	10257	4160
	PWY5F9-12	biphenyl degradation	24	0	0	0	0
Fermentation	ANAEROFRUCAT-PWY	homolactic fermentation	50064	116840	126175	94898	78485
	CENTFERM-PWY	pyruvate fermentation to butanoate	2050	30	0	10	0
	FERMENTATION-PWY	mixed acid fermentation	24537	71327	45479	34938	19004
	P108-PWY	pyruvate fermentation to propanoate I	34184	84816	60269	96896	67966
	P122-PWY	heterolactic fermentation	12101	54006	28368	23043	17358
	P163-PWY	L-lysine fermentation to acetate and butanoate	2482	16860	6883	36858	16429
	P461-PWY	hexitol fermentation to lactate, formate, ethanol and acetate	3855	14242	13124	12018	6049
	PWY-5100	pyruvate fermentation to acetate and lactate II	12730	51257	53469	58902	48133
	PWY-5676	acetyl-CoA fermentation to butanoate II	9933	51232	13936	18570	17980
	PWY-5677	succinate fermentation to butanoate	0	19	0	0	0
	PWY-6588	pyruvate fermentation to acetone	6117	26011	5485	13486	1648
	PWY-6590	superpathway of Clostridium acetobutylicum acidogenic fermentation	2580	38	0	13	0
	PWY-7111	pyruvate fermentation to isobutanol (engineered)	113541	245924	263823	179255	162532

Assimilation	CODH-PWY	reductive acetyl coenzyme A pathway	1054	501	7265	5450	0
	P23-PWY	reductive TCA cycle I	26863	58639	28021	76838	45870
	P42-PWY	incomplete reductive TCA cycle	32902	71841	57132	81655	59255
	PWY-1622	formaldehyde assimilation I (serine pathway)	5762	55706	0	2265	36317
	PWY-1861	formaldehyde assimilation II (RuMP Cycle)	14326	1901	959	60	2169
	PWY-5392	reductive TCA cycle II	0	227	255	0	0
	PWY-5744	glyoxylate assimilation	2	1253	0	0	0
Methane metabolism	METH-ACETATE-PWY	methanogenesis from acetate	1289	26	0	0	0
	METHANOGENESIS-PWY	methanogenesis from H2 and CO2	146	0	0	0	0
	PWY-1882	superpathway of C1 compounds oxidation to CO2	2671	1174	0	683	1312
Nitrogen metabolism	PWY-5705	allantoin degradation to glyoxylate III	6226	22546	30672	10063	20413
	DENITRIFICATION-PWY	nitrate reduction I (denitrification)	7192	15246	16729	17150	16161
	PWY-7084	nitrifier denitrification	36	0	0	0	0
	PWY490-3	nitrate reduction VI (assimilatory)	2894	31238	7350	5250	17021
	PWY-4984	urea cycle	27528	64489	51494	59250	35191
Oxidation	PWY-181	photorespiration	23702	85093	54962	62205	58533
	PWY-3781	aerobic respiration I (cytochrome c)	161697	302319	294644	248650	197448
	PWY-7616	methanol oxidation to carbon dioxide	2219	34316	70625	11545	30290
	RUMP-PWY	formaldehyde oxidation I	10809	1427	720	45	1631

525

530

Table A2: Relative metabolic processes [%] in lignite and incubation samples obtained using Picrust software.

Category	Pathway	]Description	Relative metabolic processes in sample [%]				
			lignite	MG	MGC	MGD	MGE
Degradation	PWY-6901	superpathway of glucose and xylose degradation	0.30	0.35	0.33	0.30	0.25
	HCAMHPDEG-PWY	3-phenylpropanoate and 3-(3-hydroxyphenyl)propanoate degradation to 2-oxopent-4-enoate	0.00	0.12	0.04	0.06	0.02
	P621-PWY	nylon-6 oligomer degradation	0.01	0.00	0.01	0.01	0.00
	PWY-5022	4-aminobutanoate degradation V	0.20	0.28	0.41	0.34	0.45
	PWY-6338	superpathway of vanillin and vanillate degradation	0.06	0.03	0.03	0.03	0.01
	PWY-6906	chitin derivatives degradation	0.00	0.01	0.01	0.00	0.00
	PWY0-41	allantoin degradation IV (anaerobic)	0.00	0.00	0.00	0.00	0.00
	P621-PWY	nylon-6 oligomer degradation	0.01	0.00	0.01	0.01	0.00
	PWY-5022	4-aminobutanoate degradation V	0.20	0.28	0.41	0.34	0.45
	PWY-6338	superpathway of vanillin and vanillate degradation	0.06	0.03	0.03	0.03	0.01
	PWY-6906	chitin derivatives degradation	0.00	0.01	0.01	0.00	0.00
	PWY0-41	allantoin degradation IV (anaerobic)	0.00	0.00	0.00	0.00	0.00
	P161-PWY	acetylene degradation	0.05	0.34	0.16	0.34	0.14
	3-HYDROXYPHENYLACETATE-DEGRADATION-PWY	4-hydroxyphenylacetate degradation	0.04	0.06	0.06	0.06	0.03
	BENZCOA-PWY	anaerobic aromatic compound degradation (Thauera aromatica)	0.00	0.00	0.00	0.00	0.00
	CATECHOL-ORTHO-CLEAVAGE-PWY	catechol degradation to β-ketoadipate	0.10	0.07	0.07	0.05	0.03
	CENTBENZCOA-PWY	benzoyl-CoA degradation II (anaerobic)	0.00	0.00	0.00	0.00	0.00
	GALACT-GLUCUROCAT-PWY	superpathway of hexuronide and hexuronate degradation	0.09	0.10	0.16	0.12	0.18
	GALLATE-DEGRADATION-I-PWY	gallate degradation II	0.12	0.14	0.09	0.13	0.01
	GALLATE-DEGRADATION-II-PWY	gallate degradation I	0.04	0.02	0.02	0.01	0.01
degradation of aromatic compounds	P184-PWY	protocatechuate degradation I (meta-cleavage pathway)	0.11	0.15	0.09	0.14	0.01

P281-PWY	3-phenylpropanoate degradation	0.15	0.28	0.27	0.29	0.22
PROTOCATECHUATE-ORTHO-CLEAVAGE-PWY	protocatechuate degradation II (ortho-cleavage pathway)	0.25	0.37	0.58	0.34	0.45
PWY-1361	benzoyl-CoA degradation I (aerobic)	0.03	0.05	0.06	0.04	0.01
PWY-5178	toluene degradation IV (aerobic) (via catechol)	0.04	0.01	0.05	0.00	0.01
PWY-5179	toluene degradation V (aerobic) (via toluene-cis-diol)	0.00	0.00	0.00	0.00	0.00
PWY-5180	toluene degradation I (aerobic) (via o-cresol)	0.05	0.22	0.11	0.22	0.09
PWY-5181	toluene degradation III (aerobic) (via p-cresol)	0.06	0.08	0.16	0.07	0.03
PWY-5182	toluene degradation II (aerobic) (via 4-methylcatechol)	0.05	0.22	0.11	0.22	0.09
PWY-5183	superpathway of aerobic toluene degradation	0.02	0.01	0.05	0.00	0.01
PWY-5184	toluene degradation VI (anaerobic)	0.00	0.00	0.00	0.00	0.00
PWY-5266	p-cymene degradation	0.03	0.00	0.00	0.00	0.00
PWY-5273	p-cumate degradation	0.03	0.00	0.00	0.00	0.00
PWY-5415	catechol degradation I (meta-cleavage pathway)	0.04	0.21	0.10	0.21	0.09
PWY-5417	catechol degradation III (ortho-cleavage pathway)	0.10	0.07	0.08	0.05	0.02
PWY-5419	catechol degradation to 2-oxopent-4-enoate II	0.02	0.01	0.04	0.03	0.00
PWY-5420	catechol degradation II (meta-cleavage pathway)	0.02	0.01	0.05	0.04	0.00
PWY-5430	meta cleavage pathway of aromatic compounds	0.01	0.00	0.04	0.02	0.00
PWY-5431	aromatic compounds degradation via β-ketoadipate	0.10	0.07	0.08	0.05	0.02
PWY-5647	2-nitrobenzoate degradation I	0.00	0.00	0.01	0.01	0.00
PWY-5654	2-amino-3-carboxymuconate semialdehyde degradation to 2-oxopentenoate	0.00	0.00	0.01	0.01	0.00
PWY-6071	superpathway of phenylethylamine degradation	0.04	0.09	0.17	0.06	0.04
PWY-6107	chlorosalicylate degradation	0.01	0.00	0.00	0.00	0.00
PWY-6182	superpathway of salicylate degradation	0.11	0.07	0.09	0.06	0.03
PWY-6185	4-methylcatechol degradation (ortho cleavage)	0.04	0.05	0.09	0.04	0.02

	PWY-6210	2-aminophenol degradation	0.00	0.00	0.01	0.01	0.00
	PWY-6339	syringate degradation	0.10	0.18	0.11	0.18	0.01
	PWY-6690	cinnamate and 3-hydroxycinnamate degradation to 2-oxopent-4-enoate	0.00	0.12	0.04	0.06	0.02
	PWY-6944	androstenedione degradation	0.00	0.08	0.03	0.02	0.00
	PWY-7046	4-coumarate degradation (anaerobic)	0.00	0.00	0.00	0.00	0.00
	PWY-7097	vanillin and vanillate degradation I	0.06	0.03	0.03	0.03	0.01
	PWY-7098	vanillin and vanillate degradation II	0.07	0.03	0.03	0.03	0.01
	PWY-722	nicotinate degradation I	0.01	0.01	0.01	0.01	0.00
	PWY-7431	aromatic biogenic amine degradation (bacteria)	0.07	0.29	0.13	0.07	0.09
	PWY0-1277	3-phenylpropanoate and 3-(3-hydroxyphenyl)propanoate degradation	0.01	0.16	0.06	0.12	0.04
	PWY0-321	phenylacetate degradation I (aerobic)	0.06	0.08	0.16	0.06	0.03
	PWY5F9-12	biphenyl degradation	0.00	0.00	0.00	0.00	0.00
Fermentation	ANAEROFRUCAT-PWY	homolactic fermentation	0.49	0.55	0.61	0.56	0.62
	CENTFERM-PWY	pyruvate fermentation to butanoate	0.02	0.00	0.00	0.00	0.00
	FERMENTATION-PWY	mixed acid fermentation	0.24	0.33	0.22	0.21	0.15
	P108-PWY	pyruvate fermentation to propanoate I	0.33	0.40	0.29	0.57	0.54
	P122-PWY	heterolactic fermentation	0.12	0.25	0.14	0.14	0.14
	P163-PWY	L-lysine fermentation to acetate and butanoate	0.02	0.08	0.03	0.22	0.13
	P461-PWY	hexitol fermentation to lactate, formate, ethanol and acetate	0.04	0.07	0.06	0.07	0.05
	PWY-5100	pyruvate fermentation to acetate and lactate II	0.12	0.24	0.26	0.35	0.38
	PWY-5676	acetyl-CoA fermentation to butanoate II	0.10	0.24	0.07	0.11	0.14
	PWY-5677	succinate fermentation to butanoate	0.00	0.00	0.00	0.00	0.00
	PWY-6588	pyruvate fermentation to acetone	0.06	0.12	0.03	0.08	0.01
	PWY-6590	superpathway of Clostridium acetobutylicum acidogenic fermentation	0.03	0.00	0.00	0.00	0.00
	PWY-7111	pyruvate fermentation to isobutanol (engineered)	1.11	1.15	1.27	1.06	1.28

Assimilation	CODH-PWY	reductive acetyl coenzyme A pathway	0.01	0.00	0.04	0.03	0.00
	P23-PWY	reductive TCA cycle I	0.26	0.27	0.14	0.45	0.36
	P42-PWY	incomplete reductive TCA cycle	0.32	0.34	0.28	0.48	0.47
	PWY-1622	formaldehyde assimilation I (serine pathway)	0.06	0.26	0.00	0.01	0.29
	PWY-1861	formaldehyde assimilation II (RuMP Cycle)	0.14	0.01	0.00	0.00	0.02
	PWY-5392	reductive TCA cycle II	0.00	0.00	0.00	0.00	0.00
	PWY-5744	glyoxylate assimilation	0.00	0.01	0.00	0.00	0.00
Methane metabolism	METH-ACETATE-PWY	methanogenesis from acetate	0.01	0.00	0.00	0.00	0.00
	METHANOGENESIS-PWY	methanogenesis from H2 and CO2	0.00	0.00	0.00	0.00	0.00
	PWY-1882	superpathway of C1 compounds oxidation to CO2	0.03	0.01	0.00	0.00	0.01
Nitrogen metabolism	PWY-5705	allantoin degradation to glyoxylate III	0.06	0.11	0.15	0.06	0.16
	DENITRIFICATION-PWY	nitrate reduction I (denitrification)	0.07	0.07	0.08	0.10	0.13
	PWY-7084	nitrifier denitrification	0.00	0.00	0.00	0.00	0.00
	PWY490-3	nitrate reduction VI (assimilatory)	0.03	0.15	0.04	0.03	0.13
	PWY-4984	urea cycle	0.27	0.30	0.25	0.35	0.28
Oxidation	PWY-181	photorespiration	0.23	0.40	0.27	0.37	0.46
	PWY-3781	aerobic respiration I (cytochrome c)	1.58	1.42	1.42	1.47	1.56
	PWY-7616	methanol oxidation to carbon dioxide	0.02	0.16	0.34	0.07	0.24
	RUMP-PWY	formaldehyde oxidation I	0.11	0.01	0.00	0.00	0.01

Author contribution

540 Conceptualization of the study was led by MB, with supervision from AS and LM. Visualisation (figures and plots) were prepared by MB and PS. The methodology, investigation and formal analysis was done by MB, PS, ADI, SD, AB, DKA, AC, DLS, AS and LM. Investigation of microbiological samples was done by PS, ADI, SD, AB, DKA, AC and AS. Geochemical study of biogas, liquids and organic matter was performed by MB, SD, DLS and LM. Funding acquisition and resources were supported by MB, DKU, DLS, AS and LM. The manuscript was wrote by MB with contribution of all co-authors.

545 **Competing interest**

The authors declare that they have no conflict of interest.

References

Alawi, M., Schneider, B., and Kallmeyer, J.: A procedure for separate recovery of extra- and intracellular DNA from a single marine sediment sample, J. Microbiol. Methods, 104, 36–42, https://doi.org/10.1016/j.mimet.2014.06.009, 2014.

555 Bag, S., Saha, B., Mehta, O., Anbumani, D., Kumar, N., Dayal, M., Pant, A., Kumar, P., Saxena, S., Allin, K. H., Hansen, T., Arumugam, M., Vestergaard, H., Pedersen, O., Pereira, V., Abraham, P., Tripathi, R., Wadhwa, N., Bhatnagar, S., Prakash, V. G., Radha, V., Anjana, R. M., Mohan, V., Takeda, K., Kurakawa, T., Nair, G. B., and Das, B.: An improved method for high quality metagenomics DNA extraction from human and environmental samples, Sci. Rep., 6, 26775, https://doi.org/10.1038/srep26775, 2016.

560 Barbera, P., Kozlov, A. M., Czech, L., Morel, B., Darriba, D., Flouri, T., and Stamatakis, A.: EPA-ng: Massively Parallel Evolutionary Placement of Genetic Sequences, Syst. Biol. 68, 365-369, https://doi.org/10.1093/sysbio/syy054, 2019.

Bechtel, A., Widera, M., and Woszczyk, M.: Composition of lipids from the First Lusatian lignite seam of the Konin Basin (Poland): Relationships with vegetation, climate and carbon cycling during the mid-Miocene Climatic Optimum, Org. Geochem., 138, 103908, https://doi.org/10.1016/j.orggeochem.2019.103908, 2019.

565   Bechtel, A., Widera, M., Lücke, A., Groß, D., and Woszczyk, M.: Petrological and geochemical characteristics of xylites and associated lipids from the First Lusatian lignite seam (Konin Basin, Poland): Implications for floral sources, decomposition and environmental conditions, Org. Geochem., 147, 104052, https://doi.org/10.1016/j.orggeochem.2020.104052, 2020.

Beck, D. A. C., Mctaggart, T. L., Setboonsarng, U., Vorobev, A., Goodwin, L., Shapiro, N., Woyke, T., Kalyuzhnaya, M. G., Lidstrom, M. E., and Chistoserdova, L.: Multiphyletic origins of methylotrophy in Alphaproteobacteria, exemplified by

570   comparative genomics of Lake Washington isolates, Environ. Microbiol., 17, 547–554, https://doi.org/10.1111/1462-2920.12736, 2015.

Berkelmann, D., Schneider, D., Meryandini, A., and Daniel, R.: Unravelling the effects of tropical land use conversion on the soil microbiome, Environ. Microbiomes, 15, 5, https://doi.org/10.1186/s40793-020-0353-3, 2020.

Bokulich, N. A., Kaehler, B. D., Rideout, J. R., Dillon, M., Bolyen, E., Knight, R., Huttley, G. A., and Gregory Caporaso, J.:

575   Optimizing taxonomic classification of marker-gene amplicon sequences with QIIME 2's q2-feature-classifier plugin, Microbiome, 6, 90, https://doi.org/10.1186/s40168-018-0470-z, 2018.

Bolyen, E., Rideout, J. R., Dillon, M. R., Bokulich, N. A., Abnet, C. C., Al-Ghalith, G. A., Alexander, H., Alm, E. J., Arumugam, M., Asnicar, F., Bai, Y., Bisanz, J. E., Bittinger, K., Brejnrod, A., Brislawn, C. J., Brown, C. T., Callahan, B. J., Caraballo-Rodríguez, A. M., Chase, J., Cope, E. K., Da Silva, R., Diener, C., Dorrestein, P. C., Douglas, G. M., Durall, D. M.,

580   Duvallet, C., Edwardson, C. F., Ernst, M., Estaki, M., Fouquier, J., Gauglitz, J. M., Gibbons, S. M., Gibson, D. L., Gonzalez, A., Gorlick, K., Guo, J., Hillmann, B., Holmes, S., Holste, H., Huttenhower, C., Huttley, G. A., Janssen, S., Jarmusch, A. K., Jiang, L., Kaehler, B. D., Kang, K. Bin, Keefe, C. R., Keim, P., Kelley, S. T., Knights, D., Koester, I., Kosciolek, T., Kreps, J., Langille, M. G. I., Lee, J., Ley, R., Liu, Y. X., Loftfield, E., Lozupone, C., Maher, M., Marotz, C., Martin, B. D., McDonald, D., McIver, L. J., Melnik, A. V., Metcalf, J. L., Morgan, S. C., Morton, J. T., Naimey, A. T., Navas-Molina, J. A., Nothias, L.

585   F., Orchanian, S. B., Pearson, T., Peoples, S. L., Petras, D., Preuss, M. L., Pruesse, E., Rasmussen, L. B., Rivers, A., Robeson, M. S., Rosenthal, P., Segata, N., Shaffer, M., Shiffer, A., Sinha, R., Song, S. J., Spear, J. R., Swafford, A. D., Thompson, L. R., Torres, P. J., Trinh, P., Tripathi, A., Turnbaugh, P. J., Ul-Hasan, S., van der Hooft, J. J. J., Vargas, F., Vázquez-Baeza, Y., Vogtmann, E., von Hippel, M.: Reproducible, interactive, scalable and extensible microbiome data science using QIIME 2, Nat. Biotechnol. 37, 852-857, https://doi.org/10.1038/s41587-019-0209-9, 2019.

590   Bucha, M., Jędrysek, M. O., Kufka, D., Pleśniak, Ł., Marynowski, L., Kubiak, K., and Błaszczyk, M.: Methanogenic fermentation of lignite with carbon-bearing additives, inferred from stable carbon and hydrogen isotopes, Int. J. Coal Geol., 186, 65–79, https://doi.org/10.1016/j.coal.2017.11.020, 2018.

Bucha, M., Detman, A., Pleśniak, Ł., Drzewicki, W., Kufka, D., Chojnacka, A., Mielecki, D., Krajniak, J., Jędrysek, M. O., Sikora, A., and Marynowski, L.: Microbial methane formation from different lithotypes of Miocene lignites from the Konin

595   Basin, Poland: Geochemistry of the gases and composition of the microbial communities, Int. J. Coal Geol., 229, https://doi.org/10.1016/j.coal.2020.103558, 2020.

Bucha, M., Lewicka-Szczebak, D., and Wójtowicz, P.: Simultaneous measurement of greenhouse gases (CH_4, CO_2 and N_2O) at atmospheric levels using a gas chromatography system, https://doi.org/10.5194/egusphere-2024-2125, 2024.

Callahan, B. J., McMurdie, P. J., Rosen, M. J., Han, A. W., Johnson, A. J. A., and Holmes, S. P.: DADA2: High-resolution
600   sample inference from Illumina amplicon data, Nat. Methods, 13, 581–583, https://doi.org/10.1038/nmeth.3869, 2016.

Caspi, R., Billington, R., Keseler, I. M., Kothari, A., Krummenacker, M., Midford, P. E., Ong, W. K., Paley, S., Subhraveti,
P., and Karp, P. D.: The MetaCyc database of metabolic pathways and enzymes-a 2019 update, Nucleic Acids. Res., 48, D455–
D453, https://doi.org/10.1093/nar/gkz862, 2020.

Chang, S. and Berner, R. A.: Coal weathering and the geochemical carbon cycle, Geochim. Cosmochim. Acta 63, 3301–3310,
605   https://doi.org/10.1016/S0016-7037(99)00252-5, 1999.

Czech, L., Barbera, P., and Stamatakis, A.: Genesis and Gappa: Processing, analyzing and visualizing phylogenetic
(placement) data, Bioinformatics, 36, 3263–3265, https://doi.org/10.1093/bioinformatics/btaa070, 2020.

Czechowski, F. and Jezierski, A.: EPR Studies on Petrographic Constituents of Bituminous Coals, Chars of Brown Coals
Group Components, and Humic Acids 600 °C Char upon Oxygen and Solvent Action, Energy Fuels, 11, 5, 951–964,
610   https://doi.org/10.1021/ef960209r, 1997.

Dai, H., Gao, J., Li, D., Wang, Z., Cui, Y., and Zhao, Y.: Family Sphingomonadaceae as the key executor of triclosan
degradation in both nitrification and denitrification systems, Chem. Eng. J., 442, 136202,
https://doi.org/10.1016/J.CEJ.2022.136202, 2022.

Deb, S., Lewicka-Szczebak, D., and Rohe, L.: Microbial nitrogen transformations tracked by natural abundance isotope studies
615   and microbiological methods: A review, Sci. Total Environ. 926, 172073, https://doi.org/10.1016/j.scitotenv.2024.172073,
2024.

Dedysh, S. N., Knief, C., and Dunfield, P. F.: Methylocella species are facultatively methanotrophic, J. Bacteriol, 187, 4665–
4670, https://doi.org/10.1128/JB.187.13.4665-4670.2005, 2005.

Detman, A., Bucha, M., Simoneit, B. R. T., Mielecki, D., Piwowarczyk, C., Chojnacka, A., Błaszczyk, M. K., Jędrysek, M.
620   O., Marynowski, L., and Sikora, A.: Lignite biodegradation under conditions of acidic molasses fermentation, Int. J. Coal
Geol., 196, 274–287, https://doi.org/10.1016/j.coal.2018.07.015, 2018.

Dey, S., Awata, T., Mitsushita, J., Zhang, D., Kasai, T., Matsuura, N., and Katayama, A.: Promotion of biological nitrogen
fixation activity of an anaerobic consortium using humin as an extracellular electron mediator, Sci. Rep., 11,
https://doi.org/10.1038/s41598-021-85955-3, 2021.

625   Douglas, G. M., Maffei, V. J., Zaneveld, J. R., Yurgel, S. N., Brown, J. R., Taylor, C. M., Huttenhower, C., and Langille, M.
G. I.: PICRUSt2 for prediction of metagenome functions, Nat. Biotechnol. 38, 685-688, https://doi.org/10.1038/s41587-020-
0548-6, 2020.

Fabiańska, M.: Organic Geochemistry of Brown Coals From the Selected Polish Basin (in Polish). University of Silesia,
Katowice. 2007.

630   Fabiańska, M. J. and Kurkiewicz, S.: Biomarkers, aromatic hydrocarbons and polar compounds in the Neogene lignites and
gangue sediments of the Konin and Turoszów Brown Coal Basins (Poland), Int. J. Coal Geol., 107, 24–44,
https://doi.org/10.1016/j.coal.2012.11.008, 2013.

Fabiańska, M. J., Ciesielczuk, J., Szczerba, M., Misz-Kennan, M., Więcław, D., Szram, E., Nádudvari, and Ciesielska, Z.: Weathering alterations of coal mining wastes geochemistry, petrography, and mineralogy, a case study from the Janina and

635 Marcel Coal Mines, Upper Silesian Coal Basin (Poland), Int. J. Coal Geol., 281, https://doi.org/10.1016/j.coal.2023.104407, 2024.

Fallgren, P. H., Jin, S., Zeng, C., Ren, Z., Lu, A., and Colberg, P. J. S.: Comparison of coal rank for enhanced biogenic natural gas production, Int. J. Coal Geol., 115, 92–96, https://doi.org/10.1016/j.coal.2013.01.014, 2013.

Finzi, A. C., Norby, R. J., Calfapietra, C., Gallet-Budynek, A., Gielen, B., Holmes, W. E., Hoosbeek, M. R., Iversen, C. M.,

640 Jackson, R. B., Kubiske, M. E., Ledford, J., Liberloo, M., Oren, R., Polle, A., Pritchard, S., Zak, D. R., Schlesinger, W. H., and Ceulemans, R.: Increases in nitrogen uptake rather than nitrogen-use efficiency support higher rates of temperate forest productivity under elevated CO_2, PNAS., 104, 14014–140192007, https://doi.org/10.1073/pnas.0706518104, 2007.

Fioretto, A., Di Nardo, C., Papa, S., and Fuggi, A.: Lignin and cellulose degradation and nitrogen dynamics during decomposition of three leaf litter species in a Mediterranean ecosystem, Soil. Biol. Biochem, 37, 1083–1091,

645 https://doi.org/10.1016/j.soilbio.2004.11.007, 2005.

Flores, R. M. and Moore, T.: Coalbed gas: A review of research directions from the past to the future as facilitated by bibliometrics, Int. J. Coal Geol., 104683, https://doi.org/10.1016/j.coal.2024.104683, 2024.

Van Groenigen, J. W., Huygens, D., Boeckx, P., Kuyper, T. W., Lubbers, I. M., Rütting, T., and Groffman, P. M.: The soil n cycle: New insights and key challenges, SOIL, 1, 235–256, https://doi.org/10.5194/soil-1-235-2015, 2015.

650 Guo, H., Yu, Z., and Zhang, H.: Phylogenetic diversity of microbial communities associated with coalbed methane gas from Eastern Ordos Basin, China, Int. J. Coal Geol., 150–151, 120–126, https://doi.org/10.1016/j.coal.2015.08.012, 2015.

Hara, S., Wada, N., Hsiao, S. S. Y., Zhang, M., Bao, Z., Iizuka, Y., Lee, D. C., Sato, S., Tang, S. L., and Minamisawa, K.: In Vivo Evidence of Single 13C and 15N Isotope–Labeled Methanotrophic Nitrogen-Fixing Bacterial Cells in Rice Roots, mBio, 13, e01255-22 https://doi.org/10.1128/mbio.01255-22, 2022.

655 Haynes, R. J.: Labile organic matter as an indicator of organic matter quality in arable and pastoral soils in New Zealand, Soil Biol. Biochem., 32, 211–219, https://doi.org/10.1016/S0038-0717(99)00148-0, 2000.

Kanehisa, M. and Goto, S.: KEGG: Kyoto Encyclopedia of Genes and Genomes, Nucleic Acids Research, 27–30 pp., 2000.

Killops, S., Killops, V.: Introduction to Organic Geochemistry. 2nd edition. Blackwell Science Ltd. USA, 2005.

Kiyohara, H., Sugiyama, M., Mondello, F.J., Gibson, D.T., Yano, K.: Plasmid Involvement In The Degradation Of Polycyclic

660 Aromatic Hydrocarbons By A *Beijerinckia* Species. Biochem. Biophys. Res. Commun. 111, 939-945, 1983.

Kwiatos, N., Jędrzejczak-Krzepkowska, M., Strzelecki, B., and Bielecki, S.: Improvement of efficiency of brown coal biosolubilization by novel recombinant Fusarium oxysporum laccase, AMB Express, 8, 1–9, https://doi.org/10.1186/s13568-018-0669-1, 2018.

Larmoia, T., Leppanen, S. M., Tuittila, E. S., Aarva, M., Merila, P., Fritze, H., and Tiirola, M.: Methanotrophy induces nitrogen

665 fixation during peatland development, Proc Natl Acad Sci U S A, 111, 734–739, https://doi.org/10.1073/pnas.1314284111, 2014.

Leschine, S.B., Holwell K., Canale-Parola, E.: Nitrogen Fixation by Anaerobic. Cellulolytic Bacteria. Science. 242, 1157–1159, 1988.

Lewicka-Szczebak, D., Jansen-Willems, A., Müller, C., Dyckmans, J., and Well, R.: Nitrite isotope characteristics and associated soil N transformations, Sci. Rep., 11, https://doi.org/10.1038/s41598-021-83786-w, 2021.

Louca, S. and Doebeli, M.: Efficient comparative phylogenetics on large trees, Bioinformatics, 34, 1053–1055, https://doi.org/10.1093/bioinformatics/btx701, 2018.

Markowicz, A., Bondarczuk, K., Wiekiera, A., and Sułowicz, S.: Is sewage sludge a valuable fertilizer? A soil microbiome and resistome study under field conditions, J. Soils Sediments, 21, 2882–2895, https://doi.org/10.1007/s11368-021-02984-1, 2021.

Martin, M.: Cutadapt removes adapter sequences from high-troughput sequencing read. J. Bioinform. 17(1), 10-12, 2011.

Marynowski, L., Bucha, M., Smolarek, J., Wendorff, M., and Simoneit, B. R. T.: Occurrence and significance of mono-, di- and anhydrosaccharide biomolecules in Mesozoic and Cenozoic lignites and fossil wood, Org Geochem, 116, 13–22, https://doi.org/10.1016/j.orggeochem.2017.11.008, 2018.

Marynowski, L., Bucha, M., Lempart-Drozd, M., Stępień, M., Kondratowicz, M., Smolarek-Lach, J., Rybicki, M., Goryl, M., Brocks, J., and Simoneit, B. R. T.: Preservation of hemicellulose remnants in sedimentary organic matter, Geochim. Cosmochim. Acta, 310, 32–46, https://doi.org/10.1016/j.gca.2021.07.003, 2021.

McDonald, D., Jiang, Y., Balaban, M., Cantrell, K., Zhu, Q., Gonzalez, A., Morton, J. T., Nicolaou, G., Parks, D. H., Karst, S. M., Albertsen, M., Hugenholtz, P., DeSantis, T., Song, S. J., Bartko, A., Havulinna, A. S., Jousilahti, P., Cheng, S., Inouye, M., Niiranen, T., Jain, M., Salomaa, V., Lahti, L., Mirarab, S., and Knight, R.: Greengenes2 unifies microbial data in a single reference tree, Nat. Biotechnol., 42, 715–718, https://doi.org/10.1038/s41587-023-01845-1, 2024.

Minamisawa, K., Imaizumi-Anraku, H., Bao, Z., Shinoda, R., Okubo, T., and Ikeda, S.: Are symbiotic methanotrophs key microbes for N acquisition in paddy rice root?, Microbes Environ, 31, 4–10, https://doi.org/10.1264/jsme2.ME15180, 2016.

Mortier, N., Velghe, F., and Verstichel, S.: Organic Recycling of Agricultural Waste Today: Composting and Anaerobic Digestion, in: Biotransformation of Agricultural Waste and By-Products: The Food, Feed, Fibre, Fuel (4F) Economy, Elsevier Inc., 69–124, https://doi.org/10.1016/B978-0-12-803622-8.00004-5, 2016.

Müller, C. and Clough, T. J.: Advances in understanding nitrogen flows and transformations: Gaps and research pathways, J. Agric. Sci. 152, S34–S44, https://doi.org/10.1017/S0021859613000610, 2014.

Müller, C., Laughlin, R. J., Spott, O., and Rütting, T.: Quantification of N_2O emission pathways via a ^{15}N tracing model, Soil Biol. Biochem., 72, 44–54, https://doi.org/10.1016/j.soilbio.2014.01.013, 2014.

Narayan, A., Jain, K., Shah, A. R., and Madamwar, D.: An efficient and cost-effective method for DNA extraction from athalassohaline soil using a newly formulated cell extraction buffer, Biotech, 6, 1–7, https://doi.org/10.1007/s13205-016-0383-0, 2016.

Nelson, P. F., Buckley, A. N., and Kelly, M. D.: Functional forms of nitrogen in coals and the release of coal nitrogen as NOx

700 precursors (HCN and NH$_3$), Symposium (International) on Combustion, 24, 1259–1267, https://doi.org/10.1016/S0082-0784(06)80148-7, 1992.

Pytlak, A., Sujak, A., Szafranek-Nakonieczna, A., Grządziel, J., Banach, A., Goraj, W., Gałązka, A., Gruszecki, W. I., and Stępniewska, Z.: Water-induced molecular changes of hard coals and lignites, Int. J. Coal Geol., 224, https://doi.org/10.1016/j.coal.2020.103481, 2020.

705 Pytlak, A., Szafranek-Nakonieczna, A., Goraj, W., Śnieżyńska, I., Krążała, A., Banach, A., Ristović, I., Słowakiewicz, M., and Stępniewska, Z.: A survey of greenhouse gases production in central European lignites, Sci. Total Environ., 800, https://doi.org/10.1016/j.scitotenv.2021.149551, 2021.

Ritter, D., Vinson, D., Barnhart, E., Akob, D. M., Fields, M. W., Cunningham, A. B., Orem, W., and McIntosh, J. C.: Enhanced microbial coalbed methane generation: A review of research, commercial activity, and remaining challenges, Int. J. Coal Geol.,

710 146, 28–41, https://doi.org/10.1016/j.coal.2015.04.013, 2015.

Rosenberg, E., Delong, E.-I.-C.E.F., Lory, S., Stackebrandt, E., Thompson, F.: The Prokaryotes. In: The Prokaryotes: Actinobacteria. 4th Edition. Springer Reference. 1–1061, 2014.

Scheffknecht, G., Al-Makhadmeh, L., Schnell, U., and Maier, J.: Oxy-fuel coal combustion-A review of the current state-of-the-art, International Journal of Greenhouse Gas Control, 5, https://doi.org/10.1016/j.ijggc.2011.05.020, 2011.

715 Schulze-Makuch, D., Wagner, D., Kounaves, S. P., Mangelsdorf, K., Devine, K. G., De Vera, J. P., Schmitt-Kopplin, P., Grossart, H. P., Parro, V., Kaupenjohann, M., Galy, A., Schneider, B., Airo, A., Frösler, J., Davila, A. F., Arens, F. L., Cáceres, L., Cornejo, F. S., Carrizo, D., Dartnell, L., DiRuggiero, J., Flury, M., Ganzert, L., Gessner, M. O., Grathwohl, P., Guan, L., Heinz, J., Hess, M., Keppler, F., Maus, D., McKay, C. P., Meckenstock, R. U., Montgomery, W., Oberlin, E. A., Probst, A. J., Sáenz, J. S., Sattler, T., Schirmack, J., Sephton, M. A., Schloter, M., Uhl, J., Valenzuela, B., Vestergaard, G., Wörmer, L., and

720 Zamorano, P.: Transitory microbial habitat in the hyperarid Atacama Desert, PNAS USA, 115, 2670–2675, https://doi.org/10.1073/pnas.1714341115, 2018.

Shi, W., Tang, S., Huang, W., Zhang, S., and Li, Z.: Distribution Characteristics of C-N-S Microorganism Genes in Different Hydraulic Zones of High-Rank Coal Reservoirs in Southern Qinshui Basin, ACS Omega, 6, 21395–21409, https://doi.org/10.1021/acsomega.1c02169, 2021.

725 Stankiewicz, B. A. and Van Bergen, P. F.: Nitrogen and N-Containing Macromolecules in the Bio-and Geosphere: An Introduction. APC Symposium Series. 797, 1-12, 2018.

Strąpoć, D., Mastalerz, M., Dawson, K., Macalady, J., Callaghan, A. V., Wawrik, B., Turich, C., Ashby, M., Strapoć, D., Mastalerz, M., Dawson, K., Macalady, J., Callaghan, A. V., Wawrik, B., Turich, C., and Ashby, M.: Biogeochemistry of microbial coal-bed methane, Annu. Rev. Earth Planet. Sci., 39, 617–656, https://doi.org/DOI 10.1146/annurev-earth-040610-

730 133343, 2011.

Tamas, I., Dedysh, S. N., Liesack, W., Stott, M. B., Alam, M., Murrell, J. C., and Dunfield, P. F.: Complete genome sequence of *Beijerinckia indica* subsp. *indica*, J. . Bacteriol. 192, 4532–4533, https://doi.org/10.1128/JB.00656-10, .2010.

Töwe, S., Wallisch, S., Bannert, A., Fischer, D., Hai, B., Haesler, F., Kleineidam, K., and Schloter, M.: Improved protocol for the simultaneous extraction and column-based separation of DNA and RNA from different soils, J. Microbiol. Methods, 84, 735 406–412, https://doi.org/10.1016/j.mimet.2010.12.028, 2011.

Vinson, D. S., Blair, N. E., Martini, A. M., Larter, S., Orem, W. H., and McIntosh, J. C.: Microbial methane from in situ biodegradation of coal and shale: A review and reevaluation of hydrogen and carbon isotope signatures, Chem. Geol., 453, 128–145, https://doi.org/10.1016/j.chemgeo.2017.01.027, 2017.

Weinstein, M. M., Prem, A., Jin, M., Tang, S., and Bhasin, J. M.: FIGARO: An efficient and objective tool for optimizing 740 microbiome rRNA gene trimming parameters, bioRxiv. 610394, https://doi.org/10.1101/610394, 2019.

Whitehead, D. L. and Quicke, G. V.: The nitrogen content of grass lignin, J. Sci. Food. Agric., 11, 151–152, https://doi.org/10.1002/jsfa.2740110306, 1960.

Widera, M.: An overview of lithotype associations of Miocene lignite seams exploited in Poland, Geologos, 22, 213–225, https://doi.org/10.1515/logos-2016-0022, 2016.

Widera, M., Kowalska, E., and Fortuna, M.: A Miocene anastomosing river system in the area of konin lignite mine, central 745 Poland, Ann. Soc. Geol. Pol. 87, 157–168., https://doi.org/10.14241/asgp.2017.012, 2017.

Ye, Y. and Doak, T. G.: A parsimony approach to biological pathway reconstruction/inference for genomes and metagenomes, PLoS Comput. Biol. 5, e1000465, https://doi.org/10.1371/journal.pcbi.1000465, 2009.

Yu, L., Harris, E., Lewicka-Szczebak, D., Barthel, M., Blomberg, M. R. A., Harris, S. J., Johnson, M. S., Lehmann, M. F., 750 Liisberg, J., Müller, C., Ostrom, N. E., Six, J., Toyoda, S., Yoshida, N., and Mohn, J.: What can we learn from N_2O isotope data? – Analytics, processes and modelling, Rapid Commun. Mass. Spectrom. 34, e8858, https://doi.org/10.1002/rcm.8858, 2020.

Yurimoto, H., Shiraishi, K., and Sakai, Y.: Physiology of methylotrophs living in the phyllosphere, Microorganisms. 9, 809, https://doi.org/10.3390/microorganisms9040809, 2021.

Zak, D. R., Holmes, W. E., Finzi, A. C., Norby, R. J., and Schlesinger, W. H.: Soil nitrogen cycling under elevated CO_2: A 755 synthesis of forest face experiments, Ecological Applications, 13, 1508–1514, https://doi.org/10.1890/03-5055, 2003.

Zhang, J., Müller, C., and Cai, Z.: Heterotrophic nitrification of organic N and its contribution to nitrous oxide emissions in soils, Soil Biol. Biochem. 84, 199-209, https://doi.org/10.1016/j.soilbio.2015.02.028, 2015.

Zieliński, T. and Widera, M.: Anastomosing-to-meandering transitional river in sedimentary record: A case study from the 760 Neogene of central Poland, Sediment. Geol., 404, https://doi.org/10.1016/j.sedgeo.2020.105677, 2020.

Zinder, S. H.: Physiological Ecology of Methanogens, Methanogenesis: Ecology, Physiology, Biochemistry and Genetics. Chapman and Hall, New York, 128–206, 1993.